TABLE I. Patient Characteristics*

No. of patients	43
No. of apheresces	104
Median (range) age in years	39 (17–63)
Sex (male/female)	29/14
Diagnosis	
NHL	31
HD	3
ALL	4
MM	1
Germinoma	3
Uterine cancer	1
Pre-PBSC chemotherapy	
Cy	14
ETP	1
Ara-C	1
Cy/ETP	22
Ara-C/MIT	1
CHOP	2
Cy/ADM/CDDP	1
ETP/CDDP/Ara-C	2
CBDCA/Ara-C/ETP/MIT	3
MTX/IFM/CBDCA/ETP	1
Median (range) no. of apheresces	2 (1–4)
Median (range) WBC count just before harvest	11,700 (3,800–47,400) μL
Median (range) no. of collected $CD34^+$ cells	0.83 (0.041–22.5) × 10^6/kg
No. who reached goal no. who received chemotherapy	
1 course	31/43
2 courses	4/5

*Abbreviations: Cy, cyclophosphamide; ETP, etoposide; Ara-C, cytosine arabinoside; MIT, mitoxantron; ADM, adriamycin; CDDP, *cis*-diamine dichloroplatinum; IFM, ifosphamide; CBDCA, carboplatin.

with the number of $CD34^+$ cells [9,24], but in our analysis there was no correlation ($r = 0.10$). In addition, no correlation was seen between the number of $CD34^+$ cells in respective harvests and the absolute reticulocyte counts ($r = 0.04$) on the day of apheresis. We also accessed the increase in WBC count on the day of apheresis as compared with the previous day and found a moderate correlation with the number of $CD34^+$ cells in respective harvests ($r = 0.46$, $P < 0.0001$, $R^2 = 0.215$).

We then assessed the correlation between the number of $CD34^+$ cells in respective harvests and differential percentages (%) on the day of apheresis. With the exception of the percentage of segmented neutrophils ($r = -0.68$), percentages of all differential components, i.e., myeloblasts, promyelocytes, myelocytes, metamyelocytes, and stabs, had a positive correlation with $CD34^+$ cell number ($r = 0.63$, 0.48, 0.76, 0.70, and 0.49, respectively). The sum of the percentages of myeloblasts, promyelocytes, myelocytes, and metamyelocytes, excluding stabs, showed a markedly high correlation ($r = 0.79$), being slightly better than that including stabs ($r = 0.77$). We therefore defined

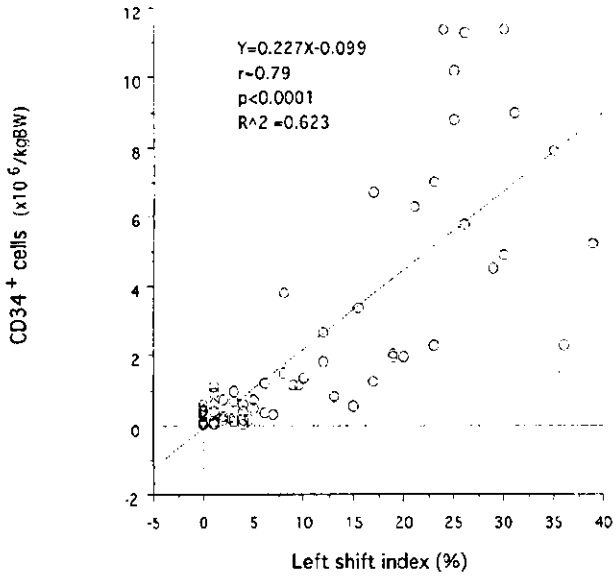

Fig. 1. Correlation analysis between Left Shift Index (LSI) and $CD34^+$ cells per apheresis product.

the former as left shift index (LSI) (Fig. 1; $r = 0.79$, $P < 0.0001$, $Y = 0.227X - 0.099$, $R^2 = 0.623$).

To render the LSI clinically usable, we evaluated ROC curves with the aim of establishing cutoff points for the optimal time to begin apheresis. The collection goal for transplantation is generally (1–2) × 10^6 $CD34^+$ cells/kg. Thus, practical goals for the number of $CD34^+$ cells from respective harvests could be 0.1 × 10^6 cells/kg, 0.25 × 10^6 cells/kg, 0.5 × 10^6 cells/kg, 1 × 10^6 cells/kg, etc. For each of the above goals, we examined ROC curves. The best cutoff point is at or near the "shoulder" of the ROC curve unless there are clinical reasons for minimizing either false negatives or false positives. According to this criterion, the best cutoff points of LSI for 0.1 × 10^6 cells/kg, 0.25 × 10^6 cells/kg, 0.5 × 10^6 cells/kg, and 1 × 10^6 cells/kg were 1.5%, 4.75%, 7.5%, and 7.5%, respectively (Fig. 2 and Table II). The cutoff point of 7.5% gives the sensitivity and specificity to obtain more than 1 × 10^6 cells/kg of 93.3% and 94.3%, respectively, meaning that only 6.7% of effective harvests are missed and only 5.6% of poor harvests will be falsely practiced. When LSI reaches more than 15.25%, nearly 100% of apheresis will attain the goal of 1 × 10^6 $CD34^+$ cells/kg. In our subjects, LSIs of 4.75%, 7.5%, and 15.25% were achieved in 35, 30, and 21 apheresis in a total of 66 apheresis trials, as summarized in Table III.

DISCUSSION

About 20–30% of patients fail to yield a sufficient number of $CD34^+$ cells to ensure prompt engraftment of neutrophils and platelets [25–29]. Apheresis failures

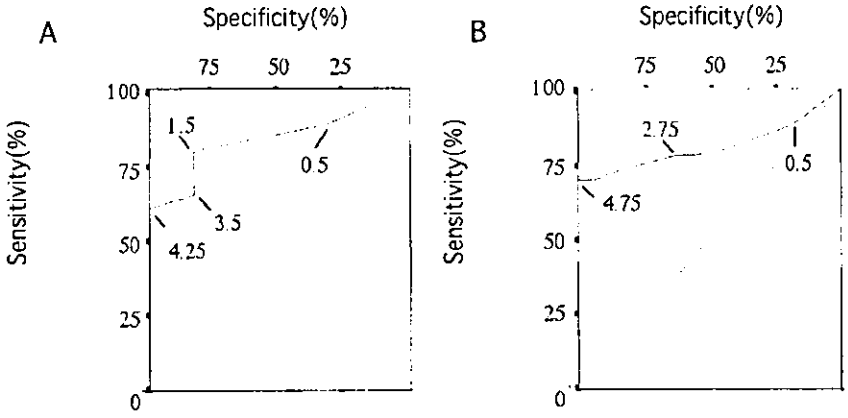

Area Under Curve	
Area	0.839
SEM	0.058
P	0.007
95% CI	72.5- 95.3%

Area Under Curve	
Area	0.810
SEM	0.051
P	0.000
95% CI	70.9- 91.1%

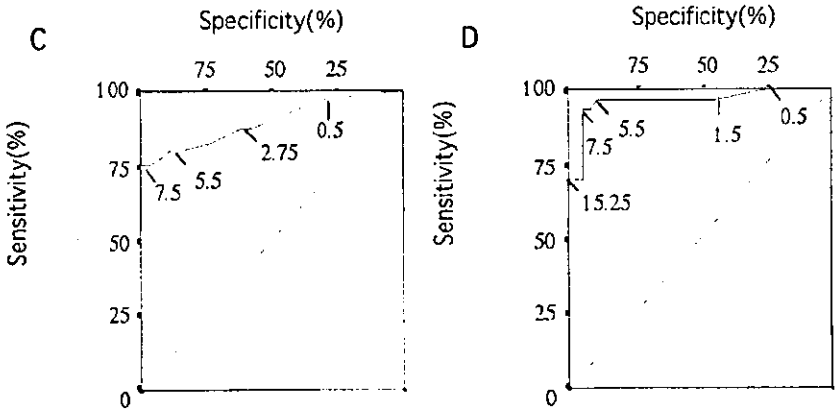

Area Under Curve	
Area	0.897
SEM	0.038
P	0.000
95% CI	82.2- 97.2%

Area Under Curve	
Area	0.962
SEM	0.025
P	0.000
95% CI	91.4-100.0%

Fig. 2. Receiver operating characteristic (ROC) curve of LSI for the prediction of sufficient or poor harvest. Target cell doses per apheresis are 0.1 × 10^6/kg BW (A), 0.25 × 10^6/kg BW (B), 0.5 × 10^6/kg BW (C), and 1.0 × 10^6/kg BW (D). Abbreviations: AUC; area under curve, SEM; standard error of the mean, P; probability, CI; confidence interval.

can be reduced if reliable indicators are available for measuring adequate mobilization of $CD34^+$ cells.

The WBC count during the recovery phase following the chemotherapy-induced nadir is widely used as the practical indicator of time to initiate apheresis, but the counts do not correlate well with the number of mobilized $CD34^+$ cells [18–20,30,31]. Several previous studies reported that the rate of WBC recovery

TABLE II. Sensitivity, Specificity, Positive, and Negative Predictive Values at the Cutoff Point of LSI in Four Kinds of Target Cell Dosage for Respective Harvest

	Target cell dosage for respective harvest (/kg BW)			
	0.1×10^6	0.25×10^6	0.5×10^6	1.0×10^6
Cutoff point of LSI (%)	1.5	4.75	7.5	7.5
Sensitivity (%)	80.0	70.0	75.0	93.3
Specificity (%)	83.3	100	100	94.3
Predictive value of positive test (%)	98.0	100	100	93.3
Predictive value of negative test (%)	29.4	51.6	72.2	94.3

TABLE III. Frequency of Achievements for the Cutoff Points of LSI

Apheresis no.	LSI > 4.75: total (%)	LSI > 7.5: total (%)	LSI > 15.25: total (%)
1st apheresis	22/33 (66.7%)	19/33 (57.6%)	13/33 (39.4%)
2nd apheresis	11/22 (50.0%)	9/22 (40.9%)	8/22 (36.4%)
3rd apheresis	2/8 (25%)	2/8 (25%)	NA
4th apheresis	0/3 (0%)	NA	NA

NA, not applicable.

could be used to predict the most effective time for apheresis [5,9,27,32,33], but in our experience, the correlation between WBC recovery rate and the $CD34^+$ cell number was moderate, indicating that this parameter is not useful in clinical practice.

Some investigators reported that pre-apheresis $CD34^+$ cell counts reliably predict $CD34^+$ cell yields. Haas et al. showed a strong correlation ($r = 0.80$) between them in 142 collections performed for 61 lymphoma patients after chemotherapy and cytokine mobilization [34]. Nevertheless, a great majority of institutions still use WBC counts or the rate of increase in the WBC count during G-SCF-assisted recovery after chemotherapy to predict the timing for optimal PBSC collection, because not all institutions have the capability to rapidly measure $CD34^+$ counts [10,11]. We could say collections have depended to empirical knowledge of clinicians in the latter institutions.

The simple sum of the percentages of immature granulocytes, proposed as LSI here, is superior to others not only in terms of its remarkably high (similar to pre-apheresis $CD34^+$ cell counts!) correlation with $CD34^+$ cell number ($r = 0.79$, $P < 0.0001$) but in terms of the adaptability to heavily pretreated patients as well. Moreover, our regression analysis has also established concrete cutoff points, which helps decisions to cease or continue collection, leads to good cost performance.

This report is a retrospective study, so we suggest that prospective studies be performed in many institutions.

ACKNOWLEDGMENTS

This work was supported in part by grants-in-aid and Special Coordination Funds for Promoting Science and Technology from the Ministry of Education, Culture, Sports, Science and Technology of Japan, and Health and Labor Sciences Research Grants (Research Grants on Pharmaceutical and Medical Safety) from the Ministry of Health, Labor and Welfare of Japan.

REFERENCES

1. Barlogie B, Shaughnessy J, Tricot G, et al. Treatment of multiple myeloma. Blood 2004;103:20–32.
2. Bender JG, Williams SF, Myers S, et al. Characterization of chemotherapy mobilized peripheral blood progenitor cells for use in autologous stem cell transplantation. Bone Marrow Transplant 1992;10:281–285.
3. Kotasek D, Shepherd KM, Sage RE, et al. Factors affecting blood stem cell collections following high-dose cyclophosphamide mobilization in lymphoma, myeloma and solid tumors. Bone Marrow Transplant 1992;9:11–17.
4. Attal M, Harousseau JL, Stoppa AM, et al. A prospective, randomized trial of autologous bone marrow transplantation and chemotherapy in multiple myeloma. Intergroupe Français du Myelome. N Engl J Med 1996;335:91–97.
5. Craig JI, Anthony RS, Stewart A, Thomson EB, Gillon J, Parker AC. Peripheral blood stem cell mobilization using high-dose cyclophosphamide and G-CSF in pretreated patients with lymphoma. Br J Haematol 1993;85:210–212.
6. Siena S, Bregni M, Brando B, et al. Flow cytometry for clinical estimation of circulating hematopoietic progenitors for autologous transplantation in cancer patients. Blood 1991;77:400–409.
7. Bensinger W, Singer J, Appelbaum F, et al. Autologous transplantation with peripheral blood mononuclear cells collected after administration of recombinant granulocyte stimulating factor. Blood 1993;81:3158–3163.
8. Hénon PH, Sovalat H, Bourderont D. Importance of $CD34^+$ cell subsets in autologous PBSC transplantation: the Mulhouse experience using $CD34^+CD38^-$ cells as predictive tool for hematopoietic engraftment. J Biol Regul Homeost Agents 2001;15:62–67.
9. Moncada V, Bolan C, Yau YY, Leitman SF. Analysis of PBPC cell yields during large-volume leukapheresis of subjects with a poor mobilization response to filgrastim. Transfusion 2003;43:495–501.
10. Elias AD, Ayash L, Anderson KC, et al. Mobilization of peripheral blood progenitor cells by chemotherapy and granulocyte-macrophage colony-stimulating factor for hematologic support after high-dose intensification for breast cancer. Blood 1992;79:3036–3044.
11. Zimmerman TM, Lee WJ, Bender JG, Mick R, Williams SF. Quantitative CD34 analysis may be used to guide peripheral blood stem cell harvests. Bone Marrow Transplant 1995;15:439–444.
12. Alegre A, Tomas JF, Martinez-Chamorro C, et al. Comparison of peripheral blood progenitor cell mobilization in patients with multiple myeloma: high-dose cyclophosphamide plus GM-CSF vs. G-CSF alone. Bone Marrow Transplant 1997;20:211–217.
13. Desikan KR, Barlogie B, Jagannath S, et al. Comparable engraftment kinetics following peripheral-blood stem-cell infusion mobilized with granulocyte colony-stimulating factor with or without cyclophosphamide in multiple myeloma. J Clin Oncol 1998;16:1547–1553.

14. Gianni AM, Siena S, Bregni M, et al. Granulocyte-macrophage colony-stimulating factor to harvest circulating haemopoietic stem cells for autotransplantation. Lancet 1989;2:580–585.
15. To LB, Shepperd KM, Haylock DN, et al. Single high doses of cyclophosphamide enable the collection of high numbers of haemopoietic stem cells from the peripheral blood. Exp Hematol 1990; 18:442–447.
16. Bensinger W, Appelbaum F, Rowley S, et al. Factors that influence collection and engraftment of autologous peripheral-blood stem cells. J Clin Oncol 1995;13:2547–2555.
17. Gordan LN, Sugrue MW, Lynch JW, et al. Poor mobilization of peripheral blood stem cells is a risk factor for worse outcome in lymphoma patients undergoing autologous stem cell transplantation. Leuk Lymphoma 2003;44:815–820.
18. Kiss JE, Rybka WB, Winkelstein A, et al. Relationship of $CD34^+$ cell dose to early and late hematopoiesis following autologous peripheral blood stem cell transplantation. Bone Marrow Transplant 1997;19:303–310.
19. Remacha AF, Martino R, Sureda A, et al. Changes in reticulocyte fractions during peripheral stem cell harvesting: role in monitoring stem cell collection. Bone Marrow Transplant 1996;17:163–168.
20. Teshima T, Harada M, Takamatsu Y, et al. Cytotoxic drug and cytotoxic drug G-CSF mobilization of peripheral blood stem cells and their use for autografting. Bone Marrow Transplant 1992;10: 215–220.
21. Morii T, Nishikawa K, Shimoyama T, et al. Quantitative flow-cytometric analysis of CD34-positive stem cells in peripheral blood stem cell harvests. Rinsho Ketsueki 1994;35:649–656 [in Japanese].
22. Miyazaki T, Matsuda I, Oguri M, et al. Flow cytometric analysis of hematopoietic progenitor cells in peripheral blood stem cell harvest from patients with CD34-positive acute leukemia. J Immunol Methods 2001;247:9–15.
23. Metz CE. Basic principles of ROC analysis. Semin Nucl Med 1978;8:283–298.
24. Okada Y, Ando M, Kato T, et al. Characteristics of blood cells during peripheral blood stem cell mobilization following chemotherapy in patients with non-Hodgkin's lymphoma. Rinsho Ketsueki 2000;41:91–96 [in Japanese].
25. Armitage S, Hargreaves R, Samson D, Brennan M, Kanfer E, Navarrete C. CD34 counts to predict the adequate collection of peripheral blood progenitor cells. Bone Marrow Transplant 1997; 20:587–591.
26. Gazitt Y, Freytes CO, Callander N, et al. Successful PBSC mobilization with high-dose G-CSF for patients failing a first round of mobilization. J Hematother 1999;8:173–183.
27. Ketterer N, Salles G, Moullet I, et al. Factors associated with successful mobilization of peripheral blood progenitor cells in 200 patients with lymphoid malignancies. Br J Haematol 1998; 103:235–242.
28. Lie AK, Hui CH, Rawling T, et al. Granulocyte colony-stimulating factor (G-CSF) dose-dependent efficacy in peripheral blood stem cell mobilization in patients who had failed initial mobilization with chemotherapy and G-CSF. Bone Marrow Transplant 1998;22:853–857.
29. Weaver CH, Tauer K, Zhen B, et al. Second attempts at mobilization of peripheral blood stem cells in patients with initial low $CD34^+$ cell yields. J Hematother 1998;7:241–249.
30. To LB, Roberts MM, Haylock DN, et al. Comparison of haematological recovery times and supportive care requirements of autologous recovery phase peripheral blood stem cell transplants, autologous bone marrow transplants and allogeneic bone marrow transplants. Bone Marrow Transplant 1992;9:277–284.
31. Yu J, Leisenring W, Bensinger WI, Holmberg LA, Rowley SD. The predictive value of white cell or $CD34^+$ cell count in the peripheral blood for timing apheresis and maximizing yield. Transfusion 1999;39:442–450.
32. Kasparu H, Krieger O, Girschikofsky M, Kolb A, Bettelheim P, Lutz D. Factors influencing the timing of peripheral blood stem cell collection (PBSC). Transfus Sci 1996;17:595–600.
33. Williams O, Demirer T, Lilleby K, Buckner CD, Bensinger WI. Tempo of hematologic recovery correlates with peripheral blood $CD34^+$ cell level in patients undergoing stem cell mobilization. J Clin Apheresis 1998;13:1–6.
34. Haas R, Mohle R, Fruhauf S, et al. Patient characteristics associated with successful mobilizing and autografting of peripheral blood progenitor cells in malignant lymphoma. Blood 1994;83:3787–3794.

THE JOURNAL OF BIOLOGICAL CHEMISTRY
Vol. 279, No. 15, Issue of April 9, pp. 15630–15638, 2004
Printed in U.S.A.

AML1 Is Functionally Regulated through p300-mediated Acetylation on Specific Lysine Residues*

Received for publication, January 13, 2004
Published, JBC Papers in Press, January 29, 2004, DOI 10.1074/jbc.M400355200

Yuko Yamaguchi‡, Mineo Kurokawa‡‖, Yoichi Imai‡, Koji Izutsu‡, Takashi Asai‡, Motoshi Ichikawa‡, Go Yamamoto‡, Eriko Nitta‡, Tetsuya Yamagata‡, Kazuki Sasaki§, Kinuko Mitani¶, Seishi Ogawa‡, Shigeru Chiba‡, and Hisamaru Hirai†‡

From the ‡Department of Hematology and Oncology, Graduate School of Medicine, University of Tokyo, Tokyo 113-8655, the §Growth Factor Division, National Cancer Center Research Institute, Tokyo 104-0045, and the ¶Department of Hematology, Dokkyo University School of Medicine, Mibu, Tochigi 321-0293, Japan

***AML1 (RUNX1)* is one of the most frequently disrupted genes in human leukemias. *AML1* encodes transcription factors, which play a pivotal role in hematopoietic differentiation, and their inappropriate expression is associated with leukemic transformation of hematopoietic cells. Previous studies demonstrated that the transcription cofactor p300 binds to the C-terminal region of AML1 and stimulates AML1-dependent transcription during myeloid cell differentiation. Here, we report that AML1 is specifically acetylated by p300 *in vitro*. Mutagenesis analyses reveal that p300 acetylates AML1 at the two conserved lysine residues (Lys-24 and Lys-43). AML1 is subject to acetylation at the same sites *in vivo*, and p300-mediated acetylation significantly augments the DNA binding activity of AML1. Disruption of these two lysines severely impairs DNA binding of AML1 and reduced the transcriptional activity and the transforming potential of AML1. Taken together, these data indicate that acetylation of AML1 through p300 is a critical manner of posttranslational modification and identify a novel mechanism for regulating the function of AML1.**

AML1 (PEBP2αB, core binding factor α2, or RUNX1) and its cofactor PEBP2β/core binding factor β are the most frequent targets of chromosomal translocations in human leukemias (1). The *AML1* gene was identified through its involvement in the (8;21) translocation, which rearranges the *AML1* gene on chromosome 21q22 and the *ETO* (*MTG8*) gene on chromosome 8q22, resulting in the generation of the AML1-ETO fusion protein (2–4). *AML1* is also involved in human leukemias carrying t(3;21) or t(12;21) translocation, suggesting that it plays an important role in leukemogenesis (5–8).

The *AML1* gene encodes a transcription factor containing an N-terminal DNA-binding domain that is highly homologous to the *Drosophila* pair-rule protein Runt, which is called the Runt domain (9). AML1 binds to the core enhancer DNA sequence, TG(T/c)GGT, called the PEBP2 site, through the Runt domain. Its affinity for DNA is markedly increased by heterodimerization with PEBP2β (10–13). This heterodimeric complex regulates transcription of a large number of hematopoietic lineage-specific genes (14, 15). Targeted disruption of either *AML1* or *PEBP2β* has demonstrated that both AML1 and PEBP2β are essential for all lineages of definitive hematopoiesis in the murine fetal liver (16–18). In addition, AML1 exhibits the transforming activity when expressed in fibroblasts, and this activity requires both the Runt domain and the C-terminal transcriptional regulatory domain called the PST region (19). At least four forms of the AML1 proteins are produced by alternative splicing, termed AML1a, AML1b, AML1c, and AML1ΔN (20, 21). Among them, AML1b is one of the transcriptionally active forms, which contain both the Runt domain and the PST region (22). We simply refer to this alternative form as AML1 hereafter.

Previously, Kitabayashi *et al.* (23) demonstrated that AML1 associates with a transcription cofactor p300 *in vivo* and that p300 potentiates AML1-dependent transcriptional activation. On the other hand, AML1 synergizes with a variety of transcription factors, including CCAAT/enhancer binding protein-α, AP-1, Ets-1, PU.1, and c-Myb, which regulate cellular proliferation and differentiation (24–30). Conversely, AML1 can repress transcription by associating with corepressors such as Groucho/transducin-like Enhancer of split and mSin3A (31–33). Thus, AML1 appears to act as an "organizing" factor of transcription by interacting with a wide variety of transcription regulators. In contrast, regulatory mechanisms for AML1 function remain elusive thus far. Previously, we reported that AML1 is phosphorylated through the extracellular signal-regulated kinase (ERK)[1] (34). ERK-dependent phosphorylation potentiates the transactivation ability and the transforming capacity of AML1 through regulating interaction between AML1 and mSin3A (35). Thus, the function of AML1 is also regulated through the signal transduction pathways.

Acetylation has recently emerged as the central mode of regulation for a significant number of transcription factors (36, 37). p300 and the related protein CBP are highly conserved proteins that have a pivotal role in transcriptional regulation, bridging a wide variety of DNA-binding proteins to components of the general transcriptional machinery (38). In addition, p300

* This work was partially supported by a fellowship from the Ministry of Education, Culture, Sports, Science and Technology of Japan. The costs of publication of this article were defrayed in part by the payment of page charges. This article must therefore be hereby marked "*advertisement*" in accordance with 18 U.S.C. Section 1734 solely to indicate this fact.

†Hisamaru Hirai died suddenly on August 23, 2003. His students, fellows, and colleagues will greatly miss his energetic and nurturing leadership in the field of hematology. We dedicate this paper in his memory.

‖ To whom correspondence should be addressed: Dept. of Hematology and Oncology, Graduate School of Medicine, University of Tokyo, 7-3-1 Hongo, Bunkyo-ku, Tokyo 113-8655, Japan. Tel.: 81-3-5800-6528; Fax: 81-3-3815-8350; E-mail: kurokawa-tky@umin.ac.jp.

[1] The abbreviations used are: ERK, extracellular signal-regulated kinase; HAT, histone acetyltransferase; GST, glutathione *S*-transferase; EMSA, electrophoretic mobility shift assay; CBP, CREB-binding protein; CREB, cAMP-response element-binding protein; luc, luciferase; PST region, a proline-, serine-, and threonine-rich region; P/CAF, p300/CBP-associated factor; M-CSF receptor, macrophage colony-stimulating factor receptor.

and CBP possess histone acetyltransferase (HAT) activity, which is able to acetylate histone and non-histone proteins. Histone acetylation is linked to transcriptional activation and participates in the nucleosomal remodeling that accompanies gene activity (39). Recently, HATs have been shown to also acetylate a significant number of non-histone proteins, which include transcription factors such as p53, *Drosophila* T-cell receptor, erythroid kruppel-like factor, GATA-1, GATA-3, and the high mobility group protein I/Y (40, 41). Acetylation of these factors leads to changes in protein-protein and protein-DNA interaction, which subsequently result in altered gene expression (42). Here we report that AML1 is acetylated by p300 at the two lysine residues located in the N terminus adjacent to the Runt domain. Acetylation of AML1 significantly increases the amount of AML1 bound to DNA and results in stimulation of AML1-dependent transcription. Substitution of target residues uncovered a close relationship between the acetylation and the *in vivo* function of AML1. Our studies demonstrate that acetylation is a critical manner of posttranslational modification of AML1.

MATERIALS AND METHODS

Cell Cultures—COS7, 293T, HeLa, and NIH3T3 cells were maintained in Dulbecco's modified Eagle's medium supplemented with penicillin, streptomycin, and 10% fetal calf serum at 37 °C in a 5% CO_2 incubator. M1 cells and MOLT-4 cells were cultured in Dulbecco's modified Eagle's medium and α-minimal essential medium by one to one and RPMI 1640 medium, respectively, which contain penicillin, streptomycin, and 10% fetal calf serum.

Plasmid Constructions and Recombinant Proteins—pGEX-AML1-(1–189), pGEX-K24R/K43R-(1–189), and pGEX-K24A/K43A-(1–189) were obtained by cloning the PCR fragments corresponding to amino acids 1–189 of AML1, K24R/K43R, and K24A/K43A into the pGEX2T vector, respectively. For construction of FLAG-tagged P/CAF-HAT/Br and GCN5, the DNA fragments corresponding to amino acids 352–832 and amino acids 1–477, respectively, were amplified by PCR and subcloned into pFLAG-MAC (Kodak). The expression plasmids for GST-PEBP2β and FLAG-tagged p300-HAT were constructed as described previously (43, 44). Construction of pME18S-AML1 and AML1Δ-(47–172) was described elsewhere (19, 45). For construction of Δ-(23–64), a fragment for amino acids 1–64 of AML1 was replaced by a fragment for amino acids 1–22 generated by a PCR method. For construction of Δ-(173–188), the ApaI-SalI fragment of AML1 was replaced by the corresponding fragment that lacks the region between amino acids 173 and 188, which was generated by a PCR method. For tagging AML1 and deletion mutants at the N terminus, the FLAG octapeptide (DYKDDDDK) was inserted after the first methionine by PCR as described previously (32). The AML1 K24R, K43R, K24R/K43R, K24A/K43A, K182R, K188R, and K182R/K188R were obtained by replacing the lysine residues with arginines and alanines, respectively, by the site-directed mutagenesis method (46). For construction of the retroviral vector that harbors AML1 or K24A/K43A, the 1.8-kb EcoRI fragment encoding AML1 or K24A/K43A was deprived of the polyadenylation signal by digestion with BamHI and cloned into the pSRαMSVtk*neo* vector (19). pM-CSF-R-luc containing −416 to +71 of the human M-CSF receptor promoter was described previously (47). pcDEF3-p300 was kindly provided by Dr. Miyazono and Dr. Kawabata. The glutathione *S*-transferase (GST) fusion constructs of AML1, FLAG-tagged p300-HAT, P/CAF-HAT/Br, and GCN5 were purified as described previously (44, 45).

In Vitro Acetylation Assays—GST fusion proteins or histones (Roche Applied Science) were collected on glutathione-Sephahrose beads (Amersham Biosciences), incubated at 30 °C for 1 h in the buffer containing 50 mM Tris, pH 8.0, 10% glycerol, 1 mM dithiothreitol, 1 mM phenylmethylsulfonyl fluoride, 10 mM sodium butyrate, and 0.05 μCi of [^{14}C]acetyl-CoA (Amersham Biosciences), and analyzed by sodium dodecyl sulfate-polyacrylamide gel electrophoresis (SDS-PAGE).

Transfection, Immunoprecipitation, and Immunoblot Analysis—COS7 cells or 293T cells were transfected with expression plasmids by the DEAE-dextran method as described previously (48). Polyclonal antisera to the full-length (anti-AML1), the PST region (anti-PST) of AML1, and PEBP2β (anti-PEBP2β) were raised in rabbit against bacterially produced proteins as described previously (43, 45, 49). For detection of p300 and AML1 proteins, the indicated cells were lysed in the buffer containing 350 mM NaCl, 50 mM Tris-HCl (pH 7.5), 0.5% Igepal, 1 mM EDTA, 0.5 mM dithiothreitol, 10 mM sodium butyrate, 1 μg of aprotinin/ml, 1 μg of pepstatin/ml, 1 μg of leupeptin/ml, 0.2 mM phenylmethylsulfonyl fluoride followed by incubation for 30 min on ice. Whole cell lysates containing 100 μg of proteins were subjected to SDS-PAGE and transferred to polyvinylidene difluoride membranes (Immobilon, Millipore). The membranes were blocked with 10% skim milk, treated with anti-p300 (RW128, Upstate Biotechnology), anti-AML1, anti-FLAG (M2; Sigma), or anti-PEBP2β, washed, and reacted with the mouse or rabbit anti-IgG antibody coupled to horseradish peroxidase. The blots were visualized using the enhanced chemiluminescence (ECL) system (Amersham Biosciences). For immunoprecipitation, cells were lysed in the above buffer and subjected to immunoprecipitation with anti-PST or anti-AML1 (PC284L; Oncogene) followed by absorption to protein A-Sepharose (Sigma). Immunoprecipitates were washed, separated by SDS-PAGE, and analyzed with anti-p300 as described above.

In Vivo Sodium [^{3}H]Acetate Labeling—MOLT-4 cells were grown to 2×10^7 cells, washed twice with cold phosphate-buffered saline, resuspended in RPMI labeling medium (1 mCi of ^{3}H-sodium acetate (Amersham Biosciences) per ml and 50 nM trichostatin A (Wako)), and then incubated at 37 °C for 90 min. pME18S-AML1 and mutants either with or without FLAG tag were transfected with pcDEF3-p300 as described above into COS7 cells. After 30 h, cells were exposed to 1 mCi of sodium [^{3}H]acetate/ml in the presence of 50 nM trichostatin A for 90 min. Lysates were prepared and processed using either anti-PST or anti-FLAG as described above and resolved by SDS-PAGE. Proteins were electrotransferred onto polyvinylidene difluoride membrane (Immobilon, Millipore) and analyzed using BAS2000 Image Analyzer (Fuji Film).

Electrophoretic Mobility Shift Assay (EMSA)—The M4 probe containing a partial A core of the polyomavirus enhancer was produced as described elsewhere (50). Five micrograms of GST fusion proteins were collected on glutathione-Sepharose beads, incubated with purified FLAG-p300-HAT in the presence or absence of 10 nM acetyl-CoA (Amersham Biosciences). Then, reaction mixtures were eluted from the beads in glutathione elution buffer (10 mM reduced glutathione in 50 mM Tris-HCl (pH 8.0)). GST-PEBP2β collected on glutathione-Sepharose beads was incubated in the thrombin (Amersham Biosciences) reaction mixture at room temperature for 16 h, and then centrifuged, and supernatant containing PEBP2β cleaved off from GST was collected. The recovered proteins were quantified by Coomassie staining, and 100 ng of these proteins were incubated with 1 ng of M4 probe in the buffer containing 20 mM Hepes (pH 7.6), 4% Ficoll (W/V), 10 mM EDTA, 40 mM KCl, 0.5 mM dithiothreitol, 300 ng of poly(dI-dC) for 30 min at room temperature in the presence or absence of PEBP2β. Seventy ng of unlabeled M4 probe were added as a cold competitor. Reaction mixtures were subjected to EMSA as described previously (45). Nuclear extracts were obtained from COS7 cells transfected with full-length AML1 or K24R/K43R in pME18S either alone or together with PEBP2β by the DEAE-dextran method, as described previously (19). The procedures for EMSA were presented previously (45). For radioisotope labeling, [α-^{32}P]dCTP was incorporated into the M4 probe by incubating with the Klenow fragment.

Luciferase Assays—HeLa cells were transfected by using SuperFect (Qiagen) with pM-CSF-R-luc and plasmids expressing wild type AML1, K24R/K43R, or K24A/K43A in the presence or absence of p300 expression plasmids. Fifty ng/ml trichostatin A was added 8 h prior to harvest. Luciferase activity was determined 48 h later, as described previously (51). A plasmid expressing β-galactosidase was co-transfected as an internal control of transfection efficiency, and the data were normalized to the β-galactosidase activity, as described previously (51).

Soft Agar Assays—Soft agar assays were performed according to procedures described elsewhere (19, 52). Colonies were counted after 14 days of culture in soft agar if they were larger than 0.25 mm in diameter.

RESULTS

AML1 Interacts with p300 in Vivo—p300 and CBP are known to interact with a variety of transcriptional factors as coactivators. Recently, a physical interaction between AML1 and p300 was demonstrated (23). To confirm the interaction of endogenous AML1 with p300 in hematopoietic cells, we performed immunoprecipitation experiments using M1 cells, a murine leukemic cell line. Whole cell lysates were prepared from M1 cells and subjected to immunoprecipitation with the anti-AML1 antibody or control preimmune serum. Immunoblot

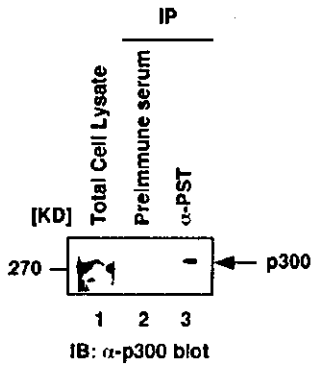

FIG. 1. **AML1 interacts with p300 *in vivo*.** Co-immunoprecipitation (*IP*) of endogenous AML1 with p300 in lysates from M1 cells is shown. Whole cell lysates were precipitated with preimmune serum (*lane 2*) or anti-PST serum (*lane 3*), and the precipitate was subjected to immunoblot (*IB*) analysis with anti-p300.

analysis with the p300-specific antibody showed that the precipitate with anti-AML1 contained p300, whereas p300 protein was never detected in the precipitate obtained with control preimmune serum (Fig. 1). These results indicate that AML1 forms complexes with p300 *in vivo* in agreement with previous findings (23).

p300 Specifically Acetylates AML1 in Vitro—Association of p300 with AML1, together with the recent demonstration of its acetyltransferase activity on a variety of transcription factors, prompted us to determine whether AML1 is a substrate for acetylation by p300. AML1 possesses nine lysine residues, which become potential targets for acetylation. To examine whether AML1 could be acetylated by p300 directly, the *in vitro* acetylation assays were performed using bacterially expressed FLAG-tagged HAT domain of p300 (p300-HAT). GST was fused to a region between amino acids 1 and 189 of AML1 (AML1-(1–189)), which contains all nine lysine residues, and the GST fusion protein was expressed in the BL21 bacterial host and purified (Fig. 2*A*). GST-AML1-(1–189) was incubated with p300-HAT in the presence of [^{14}C]acetyl-CoA. Use of these highly purified recombinant proteins eliminates possible contamination by other HATs. As shown in Fig. 2*B*, GST-AML1-(1–189) was specifically labeled with [^{14}C]acetyl-CoA in the presence of p300-HAT, whereas no signal was detected for GST alone. The faster migrating bands were considered to represent degraded products of the acetylated AML1 protein because the purified GST-AML1-(1–189) that served as a substrate contains identically migrating bands. In contrast, GST-AML1-(1–189) was never labeled without p300-HAT. We further investigated whether other HATs can acetylate AML1 using P/CAF and its close homologue GCN5. The HAT/bromodomain of P/CAF (P/CAF-HAT/Br) and full-length GCN5 were tagged with FLAG, expressed bacterially, and subsequently used in the *in vitro* acetylation assays. The results in Fig. 2*B* show that neither P/CAF-HAT/Br nor GCN5 acetylated GST-AML1-(1–189) at all. As shown in Fig. 2*C*, the HAT activities of p300-HAT, P/CAF-HAT/Br, and GCN5 were confirmed by using histones as substrates. p300-HAT could acetylate histones H2A, H2B, H3, and H4, whereas only histones H3 and H4 were acetylated by P/CAF-HAT/Br and GCN5, which is in agreement with the previous reports (42). Taken together, these results unequivocally indicate that AML1 can be a specific substrate for p300-mediated acetylation *in vitro*.

In Vivo Acetylation of AML1—Next, we went on further to examine whether acetylation of AML1 occurs *in vivo* to manifest a physiological relevance of *in vitro* acetylation of AML1. First, we wished to determine whether endogenous AML1 in hematopoietic cells was also acetylated. For these experiments, we pulse-labeled MOLT-4 cells, a human acute lymphoblastic leukemia cell line, with [^{3}H]acetate in the presence of a histone deacetylase inhibitor (trichostatin A) and then subjected them to cell lysis and immunoprecipitation with anti-AML1. As shown in Fig. 3*A*, anti-AML1, but not control preimmune serum, precipitated [^{3}H]acetate-labeled AML1 (*lanes 2* and *3*). Immunoblot analysis with the same antibody revealed migration of endogenous AML1 (*lane 1*). These results directly provide evidence that AML1 is endogenously acetylated in hematopoietic cells.

To define the positions within AML1 to be acetylated by p300, we then employed transient transfection into COS7 cells. First, cells were transfected with FLAG-tagged full-length AML1 and p300 and labeled with sodium [^{3}H]acetate in the same manner performed above. Lysates were immunoprecipitated with the anti-FLAG antibody and subjected to immunoblot analysis. As shown in Fig. 3*B*, AML1 was efficiently recovered from AML1-transfected cells with anti-FLAG. The immunoprecipitated AML1 protein was specifically labeled with [^{3}H]acetate as in MOLT-4 cells (Fig. 3*B*, *right*). Next, we employed three types of serial deletion mutants to cover all nine lysines (Fig. 2*A*). These FLAG-tagged mutants were expressed in COS7 cells together with p300 and subjected to the *in vivo* acetylation assays. Fig. 3*B* shows that these mutants are expressed in COS7 cells in the anticipated sizes. Acetylation of AML1 was retained when amino acids 47–172 in the Runt domain or amino acids 173–188 in C-terminal region adjacent to the Runt domain are deleted (*lanes 9* and *10*). In contrast, deletion of N-terminal region (amino acids 23–64) flanked by the Runt domain completely abolished AML1 acetylation by p300 (*lane 8*). This region contains two lysine residues, Lys-24 and Lys-43. These two lysines are highly conserved among the Runt-containing protein family, with Lys-24 being completely conserved from the Zebrafish Runx1 to the human AML1 family members. These results suggest that either or both of these two N-terminal lysines are potentially acetylated by p300.

AML1 Is Acetylated by p300 on N-terminal Two Lysine Residues—To precisely determine the target residues of AML1 for p300-mediated acetylation, Lys-24 and Lys-43 were substituted with arginines or alanines either individually or in combination. Substitution of either Lys-24 or Lys-43 with arginine (K24R or K43R) significantly reduced the level of acetylation. The level of acetylation in K24R was significantly lower than that in K43R. Furthermore, substitution of both Lys-24 and Lys-43 by arginines or alanines almost completely abolished acetylation of AML1 (Fig. 4*B*). In contrast, substitution of C-terminal lysines (Lys-182 and Lys-188) did not alter *in vivo* acetylation of AML1, indicating that these residues are not involved in acetylation. These findings suggest that Lys-24 and Lys-43 are preferentially acetylated *in vivo* in agreement with the results obtained from the deletion mutants. We also performed an *in vitro* acetylation assay using purified forms of GST-K24R/K43R-(1–189) and GST-K24A/K43A-(1–189) in which Lys-24 and Lys-43 of AML1-(1–189) were substituted by arginines and alanines, respectively. Although GST-AML1-(1–189) was efficiently acetylated by p300, no acetylation was detected for GST-K24R/K43R-(1–189) and GST-K24A/K43A-(1–189) (Fig. 4*C*), which is consistent with the results of the *in vivo* acetylation assays. Autoacetylated p300-HAT was observed in the very top in all lanes except the one without p300-HAT. To preclude the possibility that substitution of Lys-24 and Lys-43 can disrupt the interaction between AML1 and p300, we performed immunoprecipitation experiments by transiently expressing p300 with AML1 and K24A/K43A in 293T cells. The mutant formed a complex with p300 as effi-

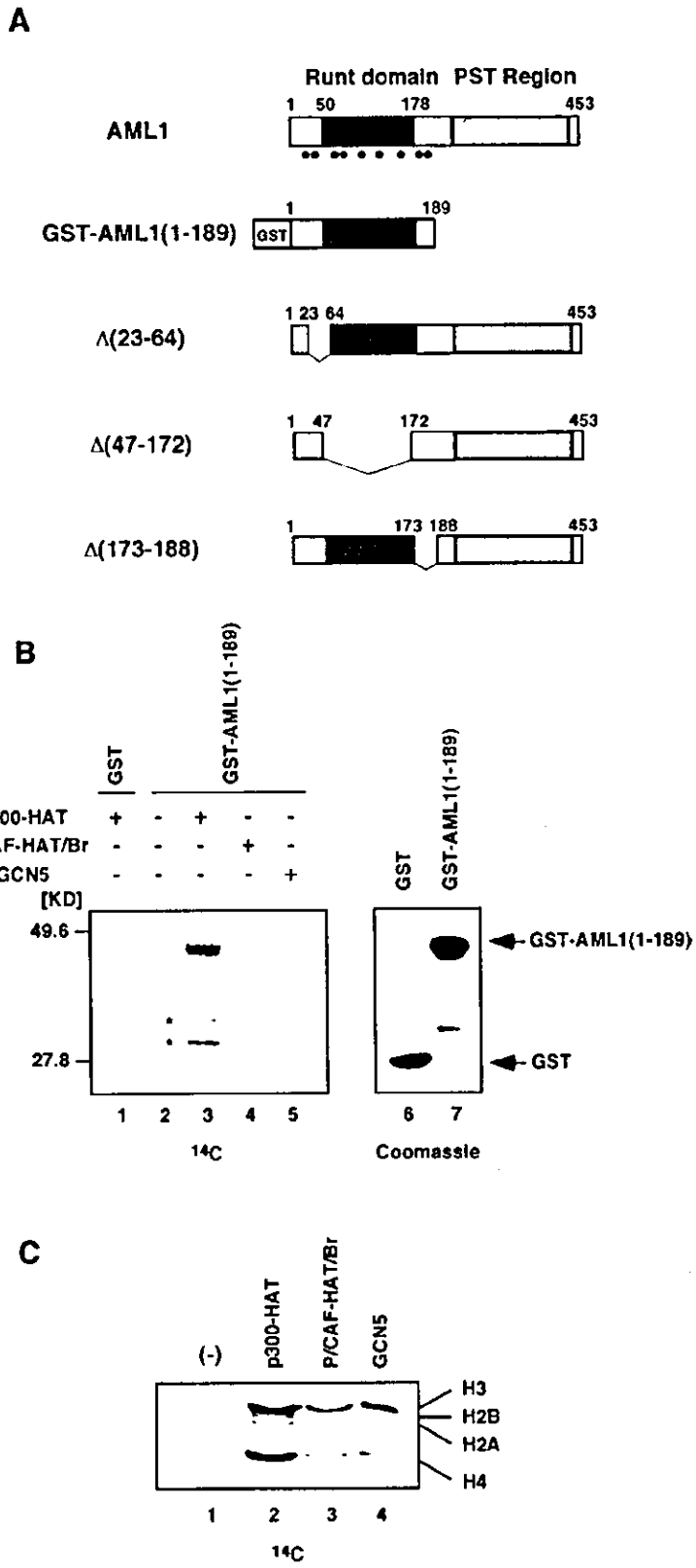

FIG. 2. ***In vitro* acetylation of AML1 by p300-HAT.** *A*, structures of AML1 and GST-AML1 fusion constructs used as substrates for p300. The Runt domain is *closed*. The PST region and GST are *shaded*. The positions of lysine residues are indicated by the *closed circles*. *B*, the *in vitro* acetylation assay of AML1 with p300-HAT, P/CAF-HAT/Br, and GCN5. Purified GST or GST-AML1-(1–189) protein was incubated with or without each recombinant HAT in the presence of [^{14}C]acetyl-CoA for 1 h at 30 °C. Reaction products were resolved by SDS-PAGE (*lanes 1–5*). The gel was stained with Coomassie Blue to demonstrate that the equivalent substrate was used in each reaction (*lanes 6* and *7*). *Asterisks* indicate degraded products of acetylated AML1. *C*, histone acetylation by various HATs. Histones (H2A, H2B, H3, and H4) were incubated either with or without each recombinant HAT in the presence of [^{14}C]acetyl-CoA for 1 h at 30 °C followed SDS-PAGE as described above.

ciently as wild type AML1 in 293T cells (data not shown). These results imply that loss of acetylation in the Lys-24/Lys-43 mutant does not result from their inability to associate with p300 but suggest that these two lysines are authentic targets for acetylation by p300.

Acetylation Augments Site-specific DNA Binding of AML1—Having identified an AML1 mutant that cannot be acetylated by p300, we set out to use this mutant to dissect the functional consequence of AML1 acetylation. For a growing number of transcription factors, it has been suggested that acetylation

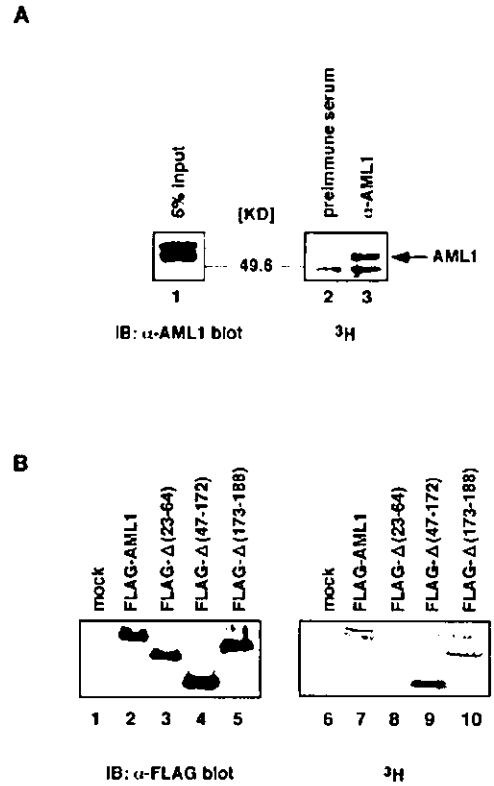

FIG. 3. **Acetylation of AML1 *in vivo*.** *A*, lysates from MOLT-4 cells pulse-labeled with 1 mCi of sodium ^{3}H/ml in the presence of 50 nM trichostatin A were immunoprecipitated with anti-AML1 or preimmune serum as a control. Immunoprecipitated samples were resolved by SDS-PAGE. Proteins were electrotransferred onto polyvinylidene difluoride membrane and immunoblotted (*IB*) with anti-AML1 (*lane 1*) or analyzed using BAS2000 image analyzer (*lanes 2* and *3*). Input represents 5% of the radiolabeled protein used in the assay. Locations of molecular mass markers and AML1 are shown. *B*, COS7 cells were transfected with 10 μg of pME18S, FLAG-tagged wild type AML1, or the FLAG-tagged deletion mutants of AML1, together with pcDEF3-p300 as indicated, and were labeled with sodium [^{3}H]acetate in the presence of trichostatin A. Whole cell lysates were immunoprecipitated with anti-PST and subsequently resolved on SDS-PAGE (*right*). Expression of each protein is monitored by immunoblotting of whole cell lysates with anti-FLAG (*left*). *mock*, mock-infected.

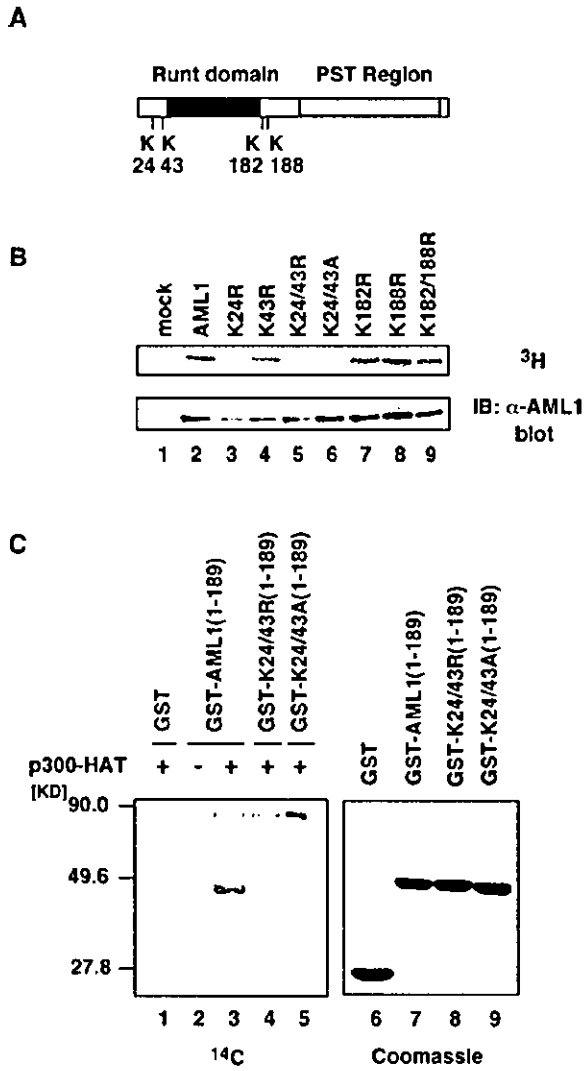

FIG. 4. **Determination of lysine residues acetylated by p300.** *A*, positions of lysine residues outside the Runt domain. *B*, the lysine mutants of AML1 were transfected into COS7 cells together with pcDEF3-p300. Transfected cells were pulse-labeled with sodium [^{3}H]acetate for 90 min. Whole cell lysates were immunoprecipitated with anti-PST and resolved by SDS-PAGE (*top*). The expression levels of each construct were monitored by immunoblotting (*IB*) of whole cell lysates with anti-AML1 (*bottom*). *mock*, mock-infected. *C*, GST fusion proteins were incubated with or without purified FLAG-tagged p300-HAT in the presence of [^{14}C]acetyl-CoA, as indicated. Reaction mixtures were separated by SDS-PAGE, fixed, and stained with Coomassie Blue (*lanes 6–9*). The stained gel was dried, and ^{14}C incorporation was visualized by BAS2000 image analyzer (*lanes 1–5*).

plays a key role in the regulation of sequence-specific DNA binding (40, 42). Since acetylation can lead to a change in the charge and the size of the lysine residues (53), it is likely that acetylation impinges on the affinity of AML1 for DNA. To test this possibility, electrophoretic mobility shift assays were performed with purified proteins for GST-AML1-(1–189) or its lysine mutant, both of which possess the Runt domain that is responsible for binding to the PEBP2 site (11, 12). Each protein was incubated with bacterially produced p300-HAT and radiolabeled M4 probe, double-stranded oligonucleotide bearing the PEBP2 site, and DNA binding abilities were evaluated. When M4 probe was incubated with GST-AML1-(1–189) and p300-HAT in the absence of acetyl-CoA, we observed a shifted band that was not seen for GST (Fig. 5*A*, *left*). The shifted band was significantly reduced when an excess of the cold probe was added, indicating that the AML1-DNA complex was formed through specific binding of AML1 to the PEBP2 sequence. We then determined the effect of p300-mediated acetylation on DNA binding of AML1. The addition of acetyl-CoA greatly augmented the shifted band (Fig. 5*A*, *left*, *lane 4*), indicating DNA binding of AML1 specifically enhanced by acetylation. In contrast, K24R/K43R substitution in GST-AML1-(1–189) significantly abolished the DNA binding ability of AML1, and no increase in DNA binding was found even upon the treatment of acetyl-CoA (Fig. 5*A*, *left*, *lanes 5* and *6*). Coomassie staining of each recombinant protein indicated the presence of equal amounts of the GST-AML1 proteins (Fig. 5*A*, *right*).

Because PEBP2β is a key regulator for DNA binding of AML1, we next tested the effect of AML1 acetylation on DNA binding in the presence of PEBP2β. As shown in Fig. 5*B* (*left*), GST-AML1-(1–189) in the presence of bacterially produced PEBP2β showed a sequence-specific DNA-binding complex that was markedly diminished by the addition of the cold probe. K24A/K43A mutation abolished the DNA binding ability of AML1 even in the presence of PEBP2β (Fig. 5*B*, *left*). The K24R/K43R mutant, which maintains the positive charge also exhibited severely impaired DNA binding, indicating that al-

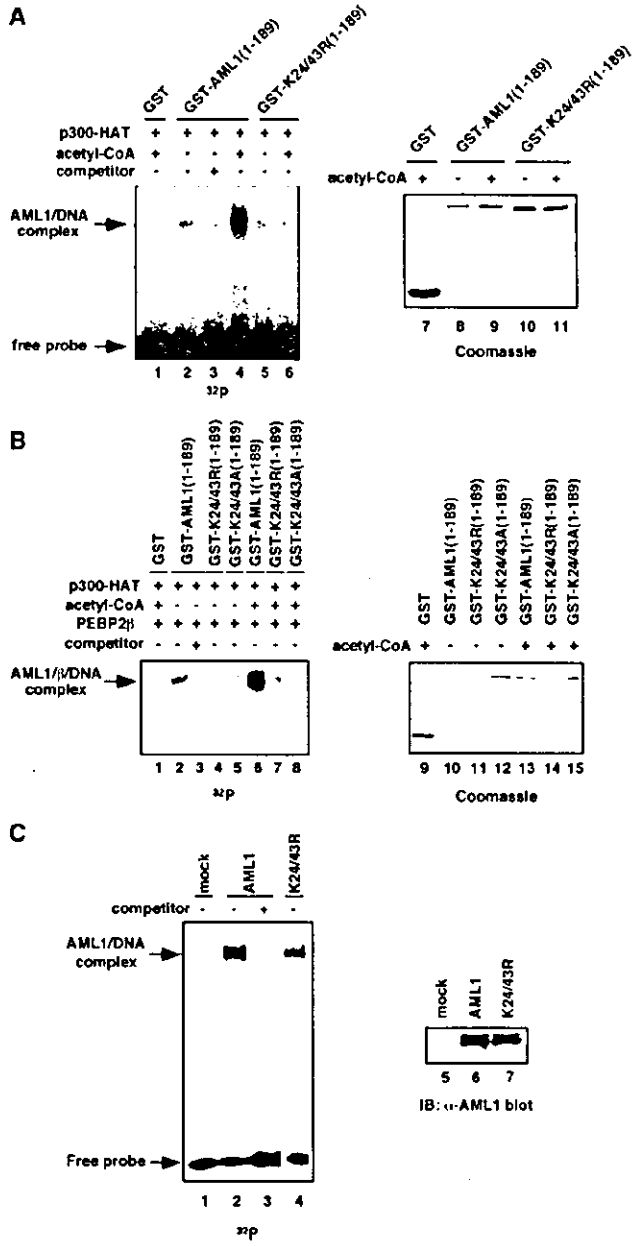

FIG. 5. **The DNA binding activity of AML1 is augmented by acetylation.** *A*, EMSAs demonstrating DNA binding of acetylated and unmodified AML1. Purified GST, GST-AML1-(1–189), or its lysine mutant (GST-K24R/K43R-(1–189)) was incubated with p300-HAT and the ^{32}P-labeled M4 probe either in the presence or in the absence of acetyl-CoA, as indicated (*left*). Excess of the unlabeled M4 probe was used as a competitor. Amounts of purified GST fusion proteins used in EMSA were monitored by Coomassie staining (*right*). *B*, DNA binding of unmodified (*lanes 2–5*) and *in vitro* acetylated GST, GST-AML1-(1–189), or its lysine mutant (GST-K24R/K43R or A-(1–189)) (*lanes 6–8*) was tested by EMSA as indicated above in the presence of bacterially expressed and purified PEBP2β (*left*). Coomassie staining exhibits the equal amounts of GST fusion proteins used in EMSA (*right*). *C*, the ^{32}P-labeled M4 probe was co-incubated with nuclear extracts (containing 18 μg of proteins) from COS7 cells co-transfected with the control vector, the wild type of full-length AML, or K24R/K43R together with PEBP2β (*left*). Expression of each protein was monitored (*right*). *IB*, immunoblot.

tered DNA binding results from a block of acetylation of Lys-24/Lys-43 rather than a fundamental change in the conformation of the mutants. Impaired DNA binding in these mutants was not restored by the addition of acetyl-CoA, which significantly enhanced DNA binding of the AML1-PEBP2β complex. Coomassie staining of each recombinant protein indicated the presence of equal amounts of the GST-AML1 proteins (Fig. 5*B*, *right*). These results indicate that PEBP2β cannot fully overcome a decrease in DNA binding of the AML1 mutants defective for acetylation.

To obtain further evidence that acetylation of target lysines alters DNA binding of AML1, we examined the effect of acetylation on sequence-specific DNA binding using full-length AML1 and its arginine mutant (K24R/K43R) in the presence of PEBP2β. We performed EMSA with nuclear extracts of COS7 cells transfected with mock, full-length AML1, and K24R/K43R together with PEBP2β. When the M4 probe was incubated and electrophoresed with nuclear extracts containing wild type AML1 in the presence of PEBP2β, a distinct band was observed that was not recognized in the lane loaded with the mock transfectant (Fig. 5*C*, *left*, *lanes 1* and *2*). This band became undetectable when a cold probe was coincubated with a labeled probe (*lane 3*), indicating that it represents a specific AML1-DNA complex. We again found that DNA binding of K24R/K43R was significantly reduced, although it still remained at a detectable level. Immunoblot analysis of nuclear extracts confirmed the presence of equal amounts of the AML1 proteins in all samples (Fig. 5*C*, *right*). Taken as a whole, these results demonstrated that DNA binding of AML1 could be regulated by acetylation of Lys-24 and Lys-43.

Heterodimerization with PEBP2β Is Not Modulated by Acetylation of AML1—The affinity of AML1 for DNA is markedly increased by heterodimerization through the Runt domain with PEBP2β, which could not interact with DNA by itself (10–13). It is possible that the altered interaction with PEBP2β could determine the DNA binding property of acetylated AML1. We asked, therefore, whether mutation of Lys-24 and Lys-43 in AML1 affects the interaction with PEBP2β. COS7 cells were transfected with wild type AML1, K24R/K43R, or K24A/K43A together with PEBP2β. The cells were lysed and immunoprecipitated with anti-PST and then subjected to immunoblot analysis using anti-PEBP2β. As shown in Fig. 6*A*, K24R/K43R and K24A/K43A associated with PEBP2β as effectively as wild type AML1. The expression level of each construct was confirmed by immunoblotting of whole cell lysates. These data indicate that Lys-24 and Lys-43, the target residues for acetylation, are dispensable for heterodimerization between AML1 and PEBP2β, suggesting that acetylation of AML1 does not affect the affinity for PEBP2β.

Acetylation by p300 Stimulates Transcriptional Activation of AML1—Because DNA binding of AML1 is stimulated in an acetylation-dependent manner, it is tempting to speculate that the transcriptional activity of AML1 can potentially be regulated by acetylation. To determine this, we examined whether substitution of Lys-24 and Lys-43 could modify transcriptional responses induced by AML1. For these experiments, we employed a reporter plasmid pM-CSF-R-luc in which the M-CSF receptor promoter is linked to the luciferase gene because it is efficiently activated by exogenous expression of AML1 (29). Wild type AML1, K24R/K43R, or K24A/K43A was introduced into HeLa cells, which lack endogenous AML1 activity, together with the reporter plasmid, and then luciferase activities were evaluated. As shown in Fig. 6*B*, we observed a 7-fold activation of pM-CSF-R-luc when wild type AML1 was expressed. In contrast, both K24R/K43R and K24A/K43A showed a significantly reduced transcriptional activation. Although p300 expression further enhanced the transcriptional activity of wild type AML1, impaired transcription by K24R/K43R and K24A/K43A was not restored even in the presence of p300. We confirmed that both K24R/K43R and K24A/K43A were ex-

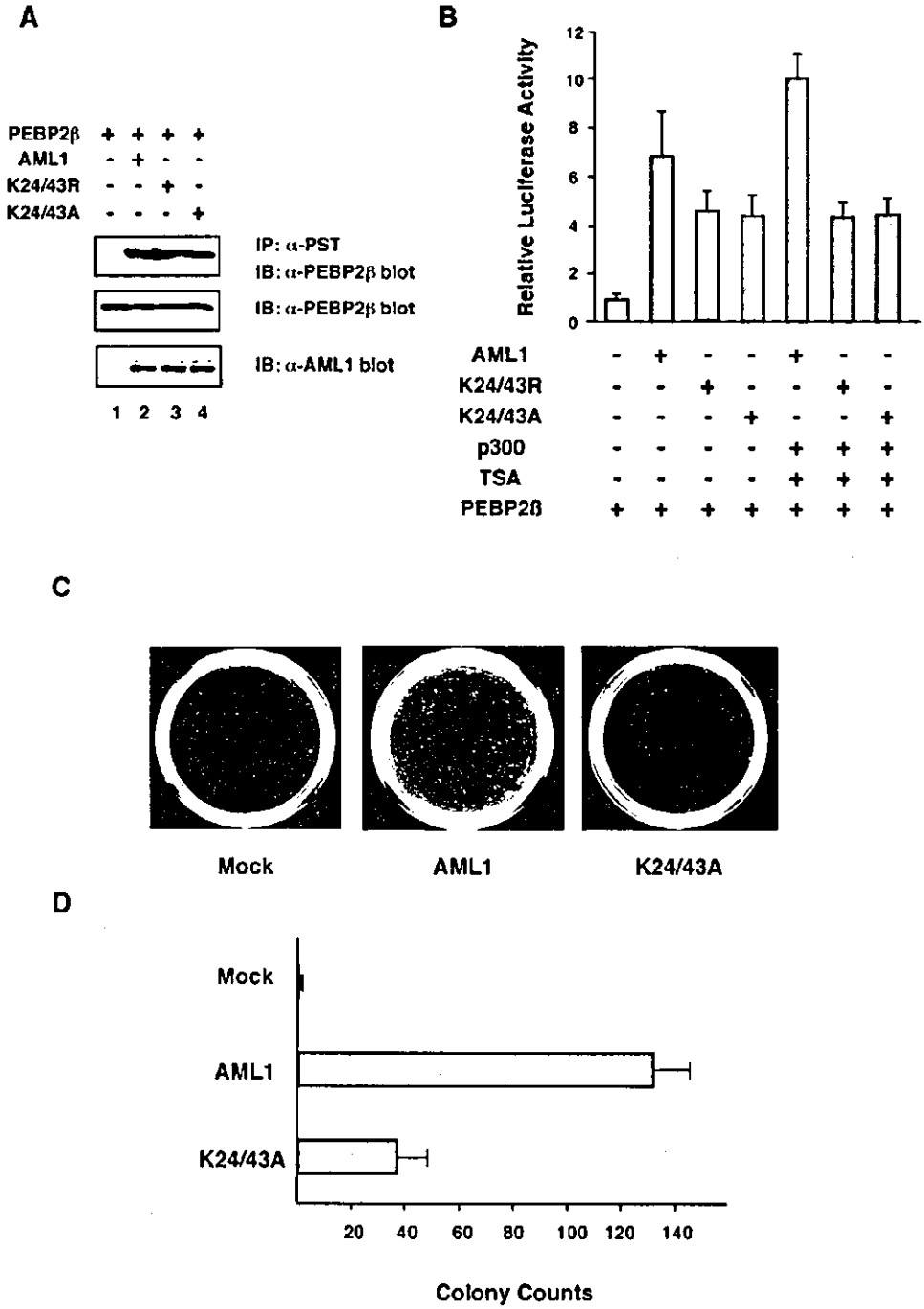

FIG. 6. *A*, interactions of wild type and the lysine mutant of AML1 with PEBP2β. COS7 cells were transfected with pME18S, wild type AML1, K24R/K43R, or K24A/K43A, together with PEBP2β as indicated. Cells were lysed, immunoprecipitated (*IP*) with anti-PST, and subjected to immunoblotting (*IB*) with anti-PEBP2β (*top*). Expression of each protein is monitored by immunoblotting of whole cell lysates with either anti-PEBP2β or anti-AML1 (*middle* and *bottom*). *B*, acetylation of AML1 stimulates its transcriptional activity. pM-CSF-R-luc was co-transfected into HeLa cells with each set of expression plasmids either with or without co-expression of p300, and the cells were analyzed for luciferase activity. Trichostatin A was added where indicated to a final concentration of 50 ng/ml at 8 h prior to harvest. Values of the relative luciferase activity and *error bars* represent the means and the standard deviations, respectively, for three independent experiments. *C*, soft agar assays with NIH3T3 cells expressing AML1 and the K24A/K43A mutant. NIH3T3 cells infected with retroviruses for AML1 or K24A/K43A of a comparable titer were seeded in soft agar after G418 selection and cultured for 14 days. Cells infected with AML1 gave larger average colony sizes and increased colony numbers, whereas cells infected with K24A/K43A created barely macroscopic colonies in agar as well as mock-infected (*mock*) cells. *D*, comparison of transforming activities of AML1 and K24A/K43A. Colonies greater than 0.25 mm in diameter were counted as positive. *Numbers* and *error bars* show the means and standard deviations of colony counts, respectively, for three independent experiments.

pressed as efficiently as wild type AML1 in HeLa cells (data not shown). These data strongly suggest that p300-mediated acetylation of AML1 on Lys-24 and Lys-43 is required for the optimal transcriptional activation of AML1.

Disruption of the Target Lysines Impairs Fibroblast-transforming Activity of AML1—Previously, we reported that overexpression of AML1 induces neoplastic transformation of NIH3T3 cells depending on the DNA binding ability and the

transcriptional activity (19). Furthermore, functional modulation of AML1 such as ERK-dependent phosphorylation significantly alters the transforming activity of AML1 (34). To study a role of acetylation in the *in vivo* function of AML1, we compared transforming activities of the wild type and the lysine mutant of AML1. Replication-deficient retroviruses for AML1 and K24A/K43A were generated by hyperexpression of the corresponding plasmid in COS7 cells. NIH3T3 cells were infected with these retroviruses, and soft agar assays were performed on G418-resistant populations. As shown in Fig. 6, *C* and *D*, wild type AML1 rapidly produced a number of macroscopic colonies in soft agar. In contrast, replacement of Lys-24 and Lys-43 to alanines remarkably impaired the transforming activity of AML1, presumably because of the inability to bind to DNA efficiently. AML1 and K24A/K43A showed equivalent expression levels in NIH3T3 cells (data not shown). These results suggest that p300-mediated acetylation on Lys-24 and Lys-43 is also important for the biological activity of AML1 *in vivo*.

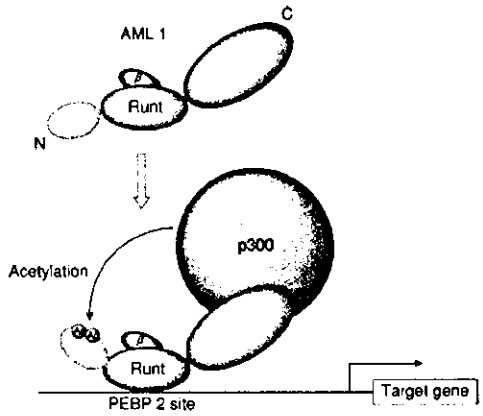

FIG. 7. **Schematic model for a regulatory mechanism of AML1 acetylation.** Physical interaction with p300 induces acetylation of AML1 at the two lysine residues in NRDBn, leading to the increase in DNA binding and transcriptional activation. NRDBn is a negative regulatory region for DNA binding N-terminal to the Runt domain.

DISCUSSION

In this study, we showed that AML1 interacts with p300 and is acetylated on the two conserved lysines in the N terminus adjacent to the Runt domain. Acetylation increases sequence-specific DNA binding of AML1 and is needed for efficient transcriptional activation by AML1. Furthermore, acetylation plays a key role for the transforming activity of AML1 in fibroblasts.

Acetylation of proteins is shown to have both stimulatory and inhibitory effects on transcription (54, 55). As for histones, acetylation is reversible and affects the strength of protein-DNA or protein-protein interactions. In addition, acetylation of several transcription factors, such as p53 and MyoD, enhances transcription of their target genes (56, 57). In contrast, acetylation of *Drosophila* T-cell receptor, high mobility group protein I/Y, and activator of thyroid and retinoic acid receptor results in decreased transcription (58–60). Thus, acetylation plays bipartite roles in the regulation of gene expression. Recently, it was reported that acetylation of E2F enhances its function via multiple mechanisms including protein half-life other than the increased DNA binding activity and transcriptional activation. These findings suggest that acetylation may affect transcription factors at multiple steps (61). In the present case, one can envision several models for the regulatory mechanisms of AML1 by acetylation. First, p300-mediated acetylation may stabilize AML1 through a prolonged protein half-life. However, we could not observe that mutation of Lys-24 and Lys-43 causes a significant difference in protein stabilization when compared with wild type (Fig. 4). Secondly, acetylation may directly increase the affinity of AML1 for DNA. Significant in this regard is our demonstration that the residues of AML1 acetylated by p300 are located in the negative regulatory region for DNA binding N-terminal to the Runt domain (NRDBn) (25, 62). It might be expected that acetylation could induce a conformational change in NRDBn that unmasks the DNA-binding interface of the Runt domain, resulting in potentiation of sequence-specific DNA binding. Schematic model for this hypothesis is shown in Fig. 7. However, Gu *et al.* (63) reported the controversial results that sequences N-terminal to the Runt domain do not affect DNA binding, which does not support this hypothesis. Another possibility is that acetylation may cause an increase in heterodimerization of AML1 with PEBP2β (25, 62). However, substitution of Lys-24 and Lys-43 does not affect the affinity of AML1 to PEBP2β, indicating that acetylation of AML1 does not contribute to heterodimerization with PEBP2β (Fig. 6*A*). Therefore, the increase in DNA binding by p300-mediated acetylation would reflect the altered interaction of AML1 itself with DNA rather than the lack of enhancing effect of the β protein. Finally, acetylation could affect protein-protein interactions, as described for binding of histone tails to the yeast transcriptional repressor Tup1 (64). Along these lines, further studies are in progress to elucidate the effect of AML1 acetylation on binding to other transcription factors such as Ets-1, CCAAT/enhancer binding protein-α, and PU.1.

In contrast to the remarkable effect of p300 acetylation on DNA binding of AML1, an impact on the transcriptional activation is relatively small. This discrepancy could be explained in several ways. First, AML1 manifests its transcriptional activation by participating in the assembly of a high order enhancer complex including other transcription factors as described above. These proteins in the complex may partially compensate for the decrease in DNA binding of AML1, which prevents a total loss of transcriptional activation. In this regard, it should be noticed that DNA binding of AML1 K24R/K43R can be detected to some extent in EMSA using nuclear extracts of COS7 cells, whereas it is much less detectable in EMSA using recombinant proteins (Fig. 5). Since many cooperating factors that associate with AML1 are supposed to exist in the nuclear extracts in contrast to highly purified recombinant proteins, it is reasonable to speculate that the formation of such a complex can partially compensate for decrease in DNA binding of AML1, which may blunt the effect of AML1 acetylation in transcriptional responses. Further investigation is needed to determine the existence of other possible intermolecular interactions. Another possibility is that other functional modifications of AML1, such as phosphorylation and methylation, may dampen the consequence of acetylation in transcriptional responses. In particular, phosphorylation is a critical modification that regulates the DNA binding activity, nuclear localization, protein interaction, and transactivation of various transcription factors. For example, p53 is phosphorylated in response to DNA damage, leading to stabilization and stimulated DNA binding *in vitro* (65, 66). Acetylation of C terminus of p53 is also observed in response to DNA damage. Furthermore, C-terminal acetylation of p53 has been shown to be regulated through its N-terminal phosphorylation induced by DNA damage, indicating an intimate cascade between phosphorylation and acetylation (56, 67, 68). Previously, we demonstrated that transcriptional activation of AML1 is regulated through phosphorylation by ERK at the specific serine residues (Ser-246 and Ser-266). Phosphorylation of AML1 is induced by cytokine stimulation in hematopoietic cells. Taken together with our present studies, it is now clear that AML1 undergoes

two types of posttranslational modifications (Fig. 7). A potential association between phosphorylation and acetylation of AML1 remains to be further investigated.

Acknowledgments—We thank M. Ohki for the gift of the human AML1 cDNAs, D. Zhang for providing the pM-CSF-R-luc vector, and Owen N Witte for the pSRαMSVtk*neo* vector and the helper virus plasmid. We also thank K. Miyazono and M. Kawabata for providing pcDEF3-p300.

REFERENCES

1. Rubnitz, J. E., and Look, A. T. (1998) *Curr. Opin. Hematol.* **5,** 264–270
2. Erickson, P., Gao, J., Chang, K. S., Look, T., Whisenant, E., Raimondi, S., Lasher, R., Trujillo, J., Rowley, J., and Drabkin, H. (1992) *Blood* **80,** 1825–1831
3. Miyoshi, H., Shimizu, K., Kozu, T., Maseki, N., Kaneko, Y., and Ohki, M. (1991) *Proc. Natl. Acad. Sci. U. S. A.* **88,** 10431–10434
4. Nisson, P. E., Watkins, P. C., and Sacchi, N. (1993) *Cancer Genet. Cytogenet.* **66,** 81
5. Mitani, K., Ogawa, S., Tanaka, T., Miyoshi, H., Kurokawa, M., Mano, H., Yazaki, Y., Ohki, M., and Hirai, H. (1994) *EMBO J.* **13,** 504–510
6. Nucifora, G., and Rowley, J. D. (1995) *Blood* **86,** 1–14
7. Romana, S. P., Mauchauffe, M., Le Coniat, M., Chumakov, I., Le Paslier, D., Berger, R., and Bernard, O. A. (1995) *Blood* **85,** 3662–3670
8. Shurtleff, S. A., Buijs, A., Behm, F. G., Rubnitz, J. E., Raimondi, S. C., Hancock, M. L., Chan, G. C., Pui, C. H., Grosveld, G., and Downing, J. R. (1995) *Leukemia (Basingstoke)* **9,** 1985–1989
9. Kania, M. A., Bonner, A. S., Duffy, J. B., and Gergen, J. P. (1990) *Genes Dev.* **4,** 1701–1713
10. Kagoshima, H., Shigesada, K., Satake, M., Ito, Y., Miyoshi, H., Ohki, M., Pepling, M., and Gergen, P. (1993) *Trends Genet.* **9,** 338–341
11. Meyers, S., Downing, J. R., and Hiebert, S. W. (1993) *Mol. Cell. Biol.* **13,** 6336–6345
12. Ogawa, E., Maruyama, M., Kagoshima, H., Inuzuka, M., Lu, J., Satake, M., Shigesada, K., and Ito, Y. (1993) *Proc. Natl. Acad. Sci. U. S. A.* **90,** 6859–6863
13. Wang, S., Wang, Q., Crute, B. E., Melnikova, I. N., Keller, S. R., and Speck, N. A. (1993) *Mol. Cell. Biol.* **13,** 3324–3339
14. Lutterbach, B., and Hiebert, S. W. (2000) *Gene (Amst.)* **245,** 223–235
15. Speck, N. A., and Terryl, S. (1995) *Crit. Rev. Eukaryotic Gene Expression* **5,** 337–364
16. Okuda, T., van Deursen, J., Hiebert, S. W., Grosveld, G., and Downing, J. R. (1996) *Cell* **84,** 321–330
17. Wang, Q., Stacy, T., Binder, M., Marin-Padilla, M., Sharpe, A. H., and Speck, N. A. (1996) *Proc. Natl. Acad. Sci. U. S. A.* **93,** 3444–3449
18. Wang, Q., Stacy, T., Miller, J. D., Lewis, A. F., Gu, T. L., Huang, X., Bushweller, J. H., Bories, J. C., Alt, F. W., Ryan, G., Liu, P. P., Wynshaw-Boris, A., Binder, M., Marin-Padilla, M., Sharpe, A. H., and Speck, N. A. (1996) *Cell* **87,** 697–708
19. Kurokawa, M., Tanaka, T., Tanaka, K., Ogawa, S., Mitani, K., Yazaki, Y., and Hirai, H. (1996) *Oncogene* **12,** 883–892
20. Miyoshi, H., Ohira, M., Shimizu, K., Mitani, K., Hirai, H., Imai, T., Yokoyama, K., Soeda, E., and Ohki, M. (1995) *Nucleic Acids Res.* **23,** 2762–2769
21. Zhang, Y. W., Bae, S. C., Huang, G., Fu, Y. X., Lu, J., Ahn, M. Y., Kanno, Y., Kanno, T., and Ito, Y. (1997) *Mol. Cell. Biol.* **17,** 4133–4145
22. Meyers, S., Lenny, N., and Hiebert, S. W. (1995) *Mol. Cell. Biol.* **15,** 1974–1982
23. Kitabayashi, I., Yokoyama, A., Shimizu, K., and Ohki, M. (1998) *EMBO J.* **17,** 2994–3004
24. Hernandez-Munain, C., and Krangel, M. S. (1995) *Mol. Cell. Biol.* **15,** 3090–3099
25. Kim, W. Y., Sieweke, M., Ogawa, E., Wee, H. J., Englmeier, U., Graf, T., and Ito, Y. (1999) *EMBO J.* **18,** 1609–1620
26. Selvamurugan, N., Chou, W. Y., Pearman, A. T., Pulumati, M. R., and Partridge, N. C. (1998) *J. Biol. Chem.* **273,** 10647–10657
27. Tenen, D. G., Hromas, R., Licht, J. D., and Zhang, D. E. (1997) *Blood* **90,** 489–519
28. Wotton, D., Ghysdael, J., Wang, S., Speck, N. A., and Owen, M. J. (1994) *Mol. Cell. Biol.* **14,** 840–850
29. Zhang, D. E., Hetherington, C. J., Meyers, S., Rhoades, K. L., Larson, C. J., Chen, H. M., Hiebert, S. W., and Tenen, D. G. (1996) *Mol. Cell. Biol.* **16,** 1231–1240
30. Zhang, D. E., Hohaus, S., Voso, M. T., Chen, H. M., Smith, L. T., Hetherington, C. J., and Tenen, D. G. (1996) *Curr. Top. Microbiol. Immunol.* **211,** 137–147
31. Aronson, B. D., Fisher, A. L., Blechman, K., Caudy, M., and Gergen, J. P. (1997) *Mol. Cell. Biol.* **17,** 5581–5587
32. Imai, Y., Kurokawa, M., Tanaka, K., Friedman, A. D., Ogawa, S., Mitani, K., Yazaki, Y., and Hirai, H. (1998) *Biochem. Biophys. Res. Commun.* **252,** 582–589
33. Lutterbach, B., Westendorf, J. J., Linggi, B., Isaac, S., Seto, E., and Hiebert, S. W. (2000) *J. Biol. Chem.* **275,** 651–656
34. Tanaka, T., Kurokawa, M., Ueki, K., Tanaka, K., Imai, Y., Mitani, K., Okazaki, K., Sagata, N., Yazaki, Y., Shibata, Y., Kadowaki, T., and Hirai, H. (1996) *Mol. Cell. Biol.* **16,** 3967–3979
35. Imai, Y., Kurokawa, M., Yamaguchi, Y., Izutsu, K., Nitta, E., Mitani, K., Satake, M., Noda, T., Ito, Y., and Hirai, H. (2004) *Mol. Cell. Biol.* **24,** 1033–1043
36. Bannister, A. J., and Kouzarides, T. (1996) *Nature* **384,** 641–643
37. Ogryzko, V. V., Schiltz, R. L., Russanova, V., Howard, B. H., and Nakatani, Y. (1996) *Cell* **87,** 953–959
38. Goodman, R. H., and Smolik, S. (2000) *Genes Dev.* **14,** 1553–1577
39. Turner, B. M. (1998) *CMLS Cell Mol. Life Sci.* **54,** 21–31
40. Bannister, A. J., and Miska, E. A. (2000) *CMLS Cell Mol. Life Sci.* **57,** 1184–1192
41. Chen, H., Tini, M., and Evans, R. M. (2001) *Curr. Opin. Cell. Biol.* **13,** 218–224
42. Sterner, D. E., and Berger, S. L. (2000) *Microbiol. Mol. Biol. Rev.* **64,** 435–459
43. Tanaka, K., Tanaka, T., Kurokawa, M., Imai, Y., Ogawa, S., Mitani, K., Yazaki, Y., and Hirai, H. (1998) *Blood* **91,** 1688–1699
44. Yamagata, T., Mitani, K., Oda, H., Suzuki, T., Honda, H., Asai, T., Maki, K., Nakamoto, T., and Hirai, H. (2000) *EMBO J.* **19,** 4676–4687
45. Tanaka, T., Tanaka, K., Ogawa, S., Kurokawa, M., Mitani, K., Nishida, J., Shibata, Y., Yazaki, Y., and Hirai, H. (1995) *EMBO J.* **14,** 341–350
46. Kunkel, T. A., Roberts, J. D., and Zakour, R. A. (1987) *Methods Enzymol.* **154,** 367–382
47. Zhang, D. E., Hetherington, C. J., Chen, H. M., and Tenen, D. G. (1994) *Mol. Cell. Biol.* **14,** 373–381
48. Tanaka, T., Mitani, K., Kurokawa, M., Ogawa, S., Tanaka, K., Nishida, J., Yazaki, Y., Shibata, Y., and Hirai, H. (1995) *Mol. Cell. Biol.* **15,** 2383–2392
49. Tanaka, K., Tanaka, T., Ogawa, S., Kurokawa, M., Mitani, K., Yazaki, Y., and Hirai, H. (1995) *Biochem. Biophys. Res. Commun.* **211,** 1023–1030
50. Furukawa, K., Yamaguchi, Y., Ogawa, E., Shigesada, K., Satake, M., and Ito, Y. (1990) *Cell Growth & Differ.* **1,** 135–147
51. Tanaka, T., Nishida, J., Mitani, K., Ogawa, S., Yazaki, Y., and Hirai, H. (1994) *J. Biol. Chem.* **269,** 24020–24026
52. Kurokawa, M., Ogawa, S., Tanaka, T., Mitani, K., Yazaki, Y., Witte, O. N., and Hirai, H. (1995) *Oncogene* **11,** 833–840
53. Martin, D. I., and Orkin, S. H. (1990) *Genes Dev.* **4,** 1886–1898
54. Imhof, A., Yang, X. J., Ogryzko, V. V., Nakatani, Y., Wolffe, A. P., and Ge, H. (1997) *Curr. Biol.* **7,** 689–692
55. Korzus, E., Torchia, J., Rose, D. W., Xu, L., Kurokawa, R., McInerney, E. M., Mullen, T. M., Glass, C. K., and Rosenfeld, M. G. (1998) *Science* **279,** 703–707
56. Sakaguchi, K., Herrera, J. E., Saito, S., Miki, T., Bustin, M., Vassilev, A., Anderson, C. W., and Appella, E. (1998) *Genes Dev.* **12,** 2831–2841
57. Sartorelli, V., Puri, P. L., Hamamori, Y., Ogryzko, V., Chung, G., Nakatani, Y., Wang, J. Y., and Kedes, L. (1999) *Mol. Cell* **4,** 725–734
58. Chakravarti, D., Ogryzko, V., Kao, H. Y., Nash, A., Chen, H., Nakatani, Y., and Evans, R. M. (1999) *Cell* **96,** 393–403
59. Munshi, N., Merika, M., Yie, J., Senger, K., Chen, G., and Thanos, D. (1998) *Mol. Cell* **2,** 457–467
60. Waltzer, L., and Bienz, M. (1998) *Nature* **395,** 521–525
61. Martinez-Balbas, M. A., Bauer, U. M., Nielsen, S. J., Brehm, A., and Kouzarides, T. (2000) *EMBO J.* **19,** 662–671
62. Ito, Y. (1999) *Genes Cells* **4,** 685–696
63. Gu, T. L., Goetz, T. L., Graves, B. J., and Speck, N. A. (2000) *Mol. Cell. Biol.* **20,** 91–103
64. Edmondson, D. G., Smith, M. M., and Roth, S. Y. (1996) *Genes Dev.* **10,** 1247–1259
65. Meek, D. W. (1998) *Cell. Signal* **10,** 159–166
66. Prives, C., and Hall, P. A. (1999) *J. Pathol.* **187,** 112–126
67. Liu, L., Scolnick, D. M., Trievel, R. C., Zhang, H. B., Marmorstein, R., Halazonetis, T. D., and Berger, S. L. (1999) *Mol. Cell. Biol.* **19,** 1202–1209
68. Luo, J., Su, F., Chen, D., Shiloh, A., and Gu, W. (2000) *Nature* **408,** 377–381

Bone Marrow Transplantation (2004) 33, 1043–1047

www.nature.com/bmt

Post-transplant complications

Predictors for severe cardiac complications after hematopoietic stem cell transplantation

M Sakata-Yanagimoto, Y Kanda, M Nakagawa, Y Asano-Mori, K Kandabashi, K Izutsu, Y Imai, A Hangaishi, M Kurokawa, S Tsujino, S Ogawa, S Chiba, T Motokura and H Hirai

Department of Cell Therapy & Transplantation Medicine, University of Tokyo, Tokyo, Japan

Summary:

The value of pre-transplant factors for predicting the development of cardiac complications after transplantation has been inconsistent among studies. We analyzed the impact of pre-transplant factors on the incidence of severe cardiac complications in 164 hematopoietic stem cell transplant recipients. We identified eight patients (4.8%) who experienced grade III or IV cardiac complications according to the Bearman criteria. Seven died of cardiac causes a median of 3 days after the onset of cardiac complications. On univariate analysis, both the cumulative dose of anthracyclines and the use of anthracyclines within 60 days before transplantation affected the incidence of severe cardiac complications ($P = 0.0091$ and 0.011). The dissociation of heart rate and body temperature, which reflects 'relative tachycardia', was also associated with a higher incidence of cardiac complications ($P = 0.024$). None of the variables obtained by electrocardiography or echocardiography were useful for predicting cardiac complications after transplantation, although the statistical power might not be sufficient to detect the usefulness of ejection fraction. On a multivariate analysis, the cumulative dose of anthracyclines was the only independent significant risk factor for severe cardiac complications. We conclude that the cumulative dose of anthracyclines is the most potent predictor of cardiac complications and the administration of anthracyclines should be avoided within two months before transplantation.

Bone Marrow Transplantation (2004) **33**, 1043–1047. doi:10.1038/sj.bmt.1704487
Published online 5 April 2004
Keywords: cardiac toxicity; stem cell transplantation; anthracycline; ejection fraction

Cardiac complications due to conditioning regimens are well recognized, and these include congestive heart failure, fatal arrhythmia, and cardiac tamponade. The incidence of such complications has varied among studies, from less than 1% to more than 26%.[1,9] The use of high-dose cyclophosphamide in the conditioning regimen has been considered to be the main cause of cardiac toxicity.[2,3,6,9] On the other hand, the usefulness of pre-transplant cardiologic evaluation for predicting cardiac complications is still controversial.[1,2,4,8,9] Braverman *et al*[3] and Fujimaki *et al*[5] showed that the incidence of severe cardiac complications was higher among patients with a low ejection fraction (EF), while Hertenstein *et al* found that there was no correlation between pre-transplant cardiac function and the development of life-threatening cardiac events.[8,9] Recently, Nakamae *et al*[8] and Akahori *et al*[5] reported that QTc dispersion and QTc interval, respectively, were good predictors for cardiac complications, which suggested that electrocardiography (ECG) before transplantation may be useful. In this study, we analyzed the impact of variables obtained by ECG and echocardiography (ultrasound cardiography; UCG) on the incidence of life-threatening cardiac complications after hematopoietic stem cell transplantation.

Patients and methods

Patients

Of the 207 adult patients who underwent hematopoietic stem cell transplantation for the first time between June 1995 and March 2003 at the University of Tokyo Hospital, Japan, we retrospectively reviewed the records of 164 patients for whom a standard 12-lead ECG and UCG within 3 months before transplantation was available. Patient characteristics are shown in Table 1. Acute leukemia in first or second remission, chronic myeloid leukemia in chronic phase, myelodysplastic syndrome with refractory anemia or refractory anemia with ringed sideroblasts, lymphoma or solid cancers in remission, and severe aplastic anemia were defined as standard-risk diseases, while others were considered high-risk diseases. In all, 132 patients underwent allogeneic transplantation, while 31 and one underwent autologous and syngeneic transplantation, respectively. Cyclophosphamide at more than 100 mg/kg was used in 129 patients (79.9%) and ifosfamide at 12 g/m^2 was used in one patient (0.6%). Total body irradiation was applied in 89 patients (54.2%).

Correspondence: Dr Y Kanda, Department of Cell Therapy & Transplantation Medicine, University of Tokyo, 7-3-1 Hongo, Bunkyo-ku, Tokyo 113-8655, Japan. E-mail: ycanda-tky@umin.ac.jp
Received 24 June 2003; accepted 8 January 2004; published online 5 April 2004

Table 1 Patient characteristics

	Severe cardiac complications		*P*-value
	Positive ($n=8$)	*Negative* ($n=156$)	
Sex (M/F)	3/5	102/54	0.14
Age > 40 years	3/8 (37.5%)	79/156 (50.6%)	0.72
Disease status (standard/high)	4/4	94/62	0.72
History of cardiac disease	0/8 (0%)	13/153 (8.4%)	>0.99
Ferritin level	738 (96.5–1379.9)	632.4 (204.9–1469.7)	0.40
Cumulative dose of anthracyclines			
Low (0–200 mg/m^2)	1	75	0.0031*
Intermediate (201–400 mg/m^2)	2	53	
High (>400 mg/m^2)	5	24	
Anthracycline within 60 days	5/8 (62.5%)	27/142 (19.0%)	0.011*
Radiation involving heart	1/8 (12.5%)	8/152 (4.6%)	0.39
ECG			
ECG abnormality	25.0%	14.7%	0.35
QT interval (ms)	370.3 (302.6–438.0)	379.1 (347.5–410.7)	0.47
QTc interval (ms)	416.4 (369.4–463.4)	424.4 (396.5–452.3)	0.45
QT dispersion (ms)	45.1 (28.2–62.0)	51.3 (30.4–72.2)	0.44
QTc dispersion (ms)	50.9 (33.3–68.5)	57.4 (34.0–80.8)	0.45
UCG			
EF (< 55%)	2/8 (25.0%)	16/142 (11.2%)	0.20
LAD (mm)	31.3 (23.5–39.1)	32.8 (26.9–38.7)	0.48
LVDd (mm)	48.0 (44.0–52.0)	48.0 (43.3–52.7)	0.99
LVDs (mm)	33.6 (28.7–38.5)	31.4 (26.9–35.9)	0.18
IVSth (mm)	8.5 (7.1–9.9)	8.8 (7.3–10.3)	0.55
PWth (mm)	8.4 (7.1–9.7)	8.6 (7.1–10.1)	0.64
E/A ratio	1.51 (0.71–2.31)	1.41 (0.83–1.99)	0.75
Vital			
Heart rate (beats/min)	80 (57–103)	76 (63–90)	0.50
Systolic blood pressure (mmHg)	108 (82–134)	112 (99–124)	0.46
HR–BT index (>25)	3/8 (37.5%)	8/138 (7.2%)	0.024*
Regimen			
Includes high-dose Cy or IFM	62.5%	80.8%	0.20
Includes TBI	4/8 (50.0%)	85/156 (54.5%)	>0.99
Stem cell			
Auto/allo	3/5	28/128	0.17
Bone marrow/peripheral blood	5/3	94/62	>0.99

*Statistically significant.

Evaluation of pre-transplant factors

QT intervals were measured manually from the beginning of the QRS complex to the end of the T wave. The average of two consecutive QT intervals was calculated as the QT interval for each lead and the QT interval for each patient was calculated as the mean QT interval of all available leads. QT dispersion was defined as the difference between the longest and shortest QT interval. Each value was corrected with Bazett's formula. QT dispersion could not be determined in three patients either because there were fewer than six readable leads ($n=2$) or due to frequent premature ventricular contractions ($n=1$).

Left ventricular EF and the E/A mitral Doppler ratio were evaluated by UCG as indices of systolic and diastolic functions, respectively. The cutoff of EF was determined as 55%, because the best *P*-value was obtained at this cutoff by univariate analyses. The following variables were also evaluated: left atrial dimension (LAD), left ventricular end-diastolic dimension (LVDd), left ventricular end-systolic dimension (LVDs), end-diastolic intraventricular septal thickness (IVth), and left ventricular posterior wall thickness (PWth).

Blood pressure, heart rate (HR), and body temperature (BT) were calculated as the means of respective values measured on 2 consecutive days prior to the conditioning regimen. The dissociation of HR and BT, called the HR–BT index, was calculated to evaluate 'relative tachycardia' as follows, assuming that the normal HR was 80 beats/min at 37°C and increased by 20 beats/min with an increase in BT of 1°C:

$$\text{HR–BT (beats/min)} = \text{HR (beats/min)} - [80 + (\text{BT (°C)} - 37) \times 20]$$

The mean HR–BT calculated from values measured on 2 consecutive days was used for the analysis.

The cumulative dose of anthracyclines was calculated as the equivalent dose of native doxorubicin, assuming that the cardiac toxicity at an equal dose is 0.5, 0.8, 3.4, 0.6, 1.6, and 0.1 for daunorubicin, pirarubicin, mitoxantrone,

epirubicin, idarubicin, and aclarubicin, respectively.[10 13] The dose of anthracyclines was then categorized into low (0–200 mg/m^2), intermediate (201–400 mg/m^2), and high (>401 mg/m^2) groups. Other potential confounding factors considered in the analysis included the history of irradiation involving the heart, presence or absence of anthracycline administration within 60 days before transplantation, and pre-transplant serum ferritin levels.

Evaluation of regimen-related cardiac toxicity

Regimen-related cardiac toxicity was graded according to Bearman grade.[2] Only cardiac complications that developed within 28 days after transplantation were considered regimen-related cardiac toxicity. Grade III–IV cardiac complications were defined to be severe.

Statistical analysis

For univariate analyses, continuous variables in the two groups were compared using the unpaired *t*-test or the Mann–Whitney *U* test, whereas categorical variables were compared using the χ^2 test or Fisher's exact test. Factors associated with at least borderline significance ($P<0.10$) on univariate analysis were subjected to a multivariate analysis using backward stepwise logistic regression. *P* values of less than 0.05 were considered statistically significant.

Results

Severe cardiac complications after transplantation

Eight patients (4.9%) developed grade III–IV cardiac complications within 28 days after transplantation (Table 1). Characteristics of the eight patients are shown in Table 2. Manifestation of cardiac complications was mainly pulmonary congestion in five (patients 1, 2, 3, 7, and 8), while two had severe hypotension (patients 4 and 5). All had primary cardiac dysfunction, not secondary to other causes. Five developed cardiac toxicity during the preparative regimen and three of them died prior to hematopoietic stem cell transplantation. The remaining three patients developed cardiac toxicity 5, 6, and 11 days after transplantation, respectively. Seven died of cardiac causes a median of 3 days (range 0–45 days) after the onset of cardiac complications.

Risk factors for severe cardiac complications

The relationships between possible confounding factors and the development of severe cardiac complications are shown in Table 1. Patient age, sex, and disease status were not associated with cardiac complications. None of the patients who developed cardiac complications had a history of cardiac disease before transplantation, while 12 of 153 patients who did not develop such complications had a prior history of cardiac disease (0% *vs* 8.4%, $P>0.99$), including angina pectoris in two, arrhythmia in six, congestive heart failure in one, leukemic infiltration of the heart in two, and surgery for tetralogy of Fallot in one. Ten patients had diabetes mellitus, five had hypertension, and one had hyperlipidemia before transplantation, but none of them developed cardiac complications after transplantation. As for prior treatments, both the cumulative dose of anthracyclines and the use of anthracyclines within 60 days before transplantation affected the incidence of severe cardiac complications ($P=0.0091$ and 0.011, respectively; Figure 1).

There was no difference in the ECG findings, including QTc interval and QTc dispersion, between those who developed severe cardiac complications and those who did

Table 2 Cardiac complications during the first 30 days

	Age/sex	*Disease status*	*Anthracycline dose (mg/m^2)*	*EF (%)*	*Conditioning regimens*	*Onset*	*Outcome (Bearman grade)*
1	30/F	ALL CR2	1054	52	ETP 40 mg/kg CY 40 mg/kg fTBI 12 Gy/6	day 5	Severe CHF (IV), died on day 31
2	42/F	AML CR2	>800	45	BU 16 mg/kg FLU 120 mg/m^2	day −3	Severe CHF (IV), died on day 36
3	27/M	NHL NR	465	55	L-PAM 140 mg/m^2 BU 8 mg/kg fTBI 12 G/6 fr	day 6	Severe CHF (IV), died on day 51
4	24/M	GCT PR	0	79	IFM 12 g/m^2 CBDCA 1600 mg/m^2 ETP 1600 mg/m^2	day −4	Cardiogenic shock, (IV), died on day -2
5	31/F	NHL CR2	384	65	CBDCA 1600 mg/m^2 ETP 1600 mg/m^2 CY 100 mg/kg AraC 4 g/m^2	day −1	Cardiogenic shock, (IV), died on day-1
6	55/M	ALL CR1	307	59	CY 120 mg/kg fTBI 12 Gy/6 fr	day −1	Cardiac tamponade, (IV), died on day 2
7	46/F	NHL NR	520	69	CBDCA 1600 mg/m^2 ETP 1600 mg/m^2 CY 100 mg/kg AraC 4 g/m^2	day −2	Severe CHF, (IV), died on day −1
8	38/F	AML CR2	408	63	CY 120 mg/kg fTBI 12 Gy/6 fr	day 11	Severe CHF, (III), alive on day 686

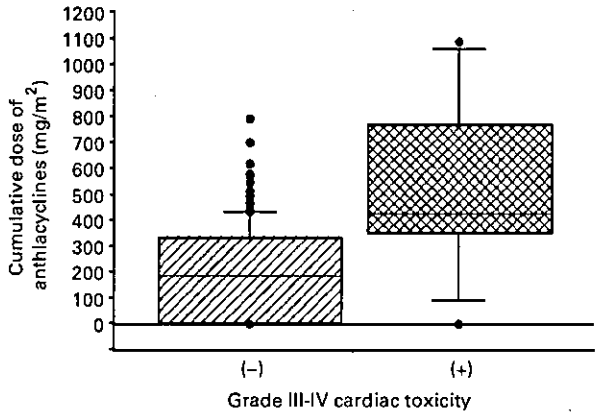

Figure 1 The cumulative dose of anthracyclines was compared in patients who developed grade III–IV cardiac complications and others. The box-and-whisker plot shows 10, 25, 50, 75, and 90 percentile values. Outliers are indicated by dots.

not. Furthermore, no difference was observed in the UCG findings, including EF and the E/A ratio, between the two groups. Impaired EF was more frequently observed in patients who developed severe cardiac complications, but the difference was not statistically significant (25% *vs* 11.2%, $P=0.25$). Heart rate and systolic blood pressure before transplantation were not correlated with the incidence of severe cardiac complications. However, a high HR–BT index, which reflected 'relative tachycardia', was associated with a higher incidence of cardiac complications (37.5% *vs* 7.2%, $P=0.024$).

The use of high-dose cyclophosphamide or ifosfamide was less frequent in patients who developed severe cardiac complications. This may have been because high-dose cyclophosphamide tended to be avoided in patients who were considered to be at higher risk for severe cardiac complications. The use of TBI did not affect the incidence of cardiac complications ($P>0.99$).

By multivariate analysis, the cumulative dose of anthracyclines was identified as the only independent significant risk factor for severe cardiac complications, with an odds ratio of 4.33 (95% CI 1.48–12.7, $P=0.0075$) for changes between categories.

Discussion

Cardiac toxicity due to the conditioning regimen is a well-recognized complication after hematopoietic stem cell transplantation.[2,3,9] The incidence of severe cardiac complications was 4.9% in this series, which is consistent with the values in previous reports (0.9%–26%).[1,9] We found that the cumulative dose of anthracyclines correlated independently with the development of grade III–IV cardiac complications. Five of the 29 patients (17.2%) who had received more than 400 mg/m^2 of anthracyclines developed severe cardiac complications. Furthermore, among this population, four of the 12 patients (33%) who had received anthracyclines within 60 days before transplantation developed severe cardiac complications, whereas these were seen in only one of 14 patients (7.1%) who had not received anthracyclines within 60 days, although this difference was not statistically significant ($P=0.15$).

The predictive value of pre-transplant cardiac evaluation has been inconsistent among studies. Braverman *et al* and Fujimaki *et al* showed that a reduced pre-transplant EF could be a predictive factor,[3,5] while Hertenstein *et al* showed that the incidence of life-threatening cardiac toxicity was not significantly increased in patients with reduced EF.[9] In this study, the incidence of severe cardiac toxicity was higher in the reduced EF (<55%) group, but this difference was not statistically significant (11.1% *vs* 4.5%, $P=0.25$). It is possible that the number of patients was too small to detect the difference; the statistical power of this study to detect the difference was only 15%. In addition, we tended to use less toxic regimens for patients with a reduced pre-transplant EF. This might also explain why a high-dose cyclophosphamide regimen was used less frequently in patients who developed severe cardiac complications.

In this study, we closely analyzed the correlation between severe cardiac complications and variables obtained by ECG or UCG, but none were useful for predicting cardiac complications after transplantation, although the usefulness of EF should not be excluded. On the other hand, relative tachycardia as shown by a high HR–BT index may reflect reduced cardiac reserve. In fact, a high HR–BT was associated with a higher incidence of severe cardiac complications on univariate analysis. Although this was not confirmed by multivariate analysis, it may be worthwhile to further evaluate the impact of this variable, since the HR–BT index can be determined easily without any cost. As another marker for cardiac reserve, Zangari *et al* showed that the increment of EF during excise was useful to predict overall peritransplant mortality, suggesting that pre-transplant cardiac reserve may be important in predicting transplant outcome.[14]

In conclusion, patients who had received a high cumulative dose of anthracyclines, particularly more than 400 mg/m^2, were at the highest risk for severe cardiac complications. Clinical interventions to prevent cardiac toxicity, such as the use of reduced-intensity conditioning or angiotensin-converting enzyme inhibitor as a cardioprotectant, should be evaluated in such patients.[15] Also, the administration of anthracyclines should be avoided within 2 months before transplantation.

References

1 Akahori M, Nakamae H, Hino M *et al.* Electrocardiogram is very useful for predicting acute heart failure following myeloablative chemotherapy with hematopoietic stem cell transplantation rescue. *Bone Marrow Transplant* 2003; **31**: 585–590.

2 Bearman SI, Petersen FB, Schor RA *et al.* Radionuclide ejection fractions in the evaluation of patients being considered for bone marrow transplantation: risk for cardiac toxicity. *Bone Marrow Transplant* 1990; **5**: 173–177.

3 Braverman AC, Antin JH, Plappert MT *et al.* Cyclophosphamide cardiotoxicity in bone marrow transplantation: a

prospective evaluation of new dosing regimens. *J Clin Oncol* 1991; **9**: 1215–1223.
4 Brockstein BE, Smiley C, Al-Sadir J *et al.* Cardiac and pulmonary toxicity in patients undergoing high-dose chemotherapy for lymphoma and breast cancer: prognostic factors. *Bone Marrow Transplant* 2000; **25**: 885–894.
5 Fujimaki K, Maruta A, Yoshida M *et al.* Severe cardiac toxicity in hematological stem cell transplantation: predictive value of reduced left ventricular ejection fraction. *Bone Marrow Transplant* 2001; **27**: 307–310.
6 Goldberg MA, Antin JH, Guinan EC *et al.* Cyclophosphamide cardiotoxicity: an analysis of dosing as a risk factor. *Blood* 1986; **68**: 1114–1118.
7 Murdych T, Weisdorf DJ. Serious cardiac complications during bone marrow transplantation at the University of Minnesota, 1977–1997. *Bone Marrow Transplant* 2001; **28**: 283–287.
8 Nakamae H, Tsumura K, Hino M *et al.* QT dispersion as a predictor of acute heart failure after high-dose cyclophosphamide. *Lancet* 2000; **355**: 805–806.
9 Hertenstein B, Stefanic M, Schmeiser T *et al.* Cardiac toxicity of bone marrow transplantation: predictive value of cardiologic evaluation before transplant. *J Clin Oncol* 1994; **12**: 998–1004.
10 Herait P, Poutignat N, Marty M *et al.* Early assessment of a new anticancer drug analogue—are the historical comparisons obsolete? The French experience with pirarubicin. *Eur J Cancer* 1992; **28A**: 1670–1676.
11 Casazza AM, Savi G, Pratesi G *et al.* Antitumor activity in mice of 4′-deoxydoxorubicin in comparison with doxorubicin. *Eur J Cancer Clin Oncol* 1983; **19**: 411–418.
12 Hori S, Shirai M, Hirano S *et al.* Antitumor activity of new anthracycline antibiotics, aclacinomycin-A and its analogs, and their toxicity. *Gann* 1977; **68**: 685–690.
13 Anderlini P, Benjamin RS, Wong FC *et al.* Idarubicin cardiotoxicity: a retrospective study in acute myeloid leukemia and myelodysplasia. *J Clin Oncol* 1995; **13**: 2827–2834.
14 Zangari M, Henzlova MJ, Ahmad S *et al.* Predictive value of left ventricular ejection fraction in stem cell transplantation. *Bone Marrow Transplant* 1999; **23**: 917–920.
15 Kakavas PW, Ghalie R, Parrillo JE *et al.* Angiotensin converting enzyme inhibitors in bone marrow transplant recipients with depressed left ventricular function. *Bone Marrow Transplant* 1995; **15**: 859–861.

Bone Marrow Transplantation (2004) 33, 549–552

www.nature.com/bmt

Graft-versus-host disease

Increased incidence of acute graft-versus-host disease with the continuous infusion of cyclosporine A compared to twice-daily infusion

N Ogawa, Y Kanda, M Matsubara, Y Asano, M Nakagawa, M Sakata-Yanagimoto, K Kandabashi, K Izutsu, Y Imai, A Hangaishi, M Kurokawa, S Tsujino, S Ogawa, K Aoki, S Chiba, T Motokura and H Hirai

Department of Cell Therapy and Transplantation Medicine, University of Tokyo, Bunkyo-ku, Tokyo, Japan

Summary:

We retrospectively compared the incidence of acute graft-versus-host disease (GVHD) before and after September 1999, when we changed the mode of cyclosporine A (CsA) administration from twice-daily infusions (TD) ($n = 58$) to continuous infusion (CIF) ($n = 71$). The incidence of grade II–IV acute GVHD in the CIF group (56%) was significantly higher than that in the TD group (27%, $P = 0.00022$). Multivariate analysis identified only two independent significant risk factors for the development of grade II–IV acute GVHD; CIF of CsA (relative risk 2.59, 95% CI 1.46–4.60, $P = 0.0011$) and the presence of HLA mismatch (2.01, 95% CI 1.15–3.53, $P = 0.014$). The incidence of relapse was significantly lower in the CIF group when adjusted for disease status before transplantation (0.41, 95% CI 0.18–0.95, $P = 0.038$), which resulted in better disease-free survival in high-risk patients (43 *vs* 16% at 2 years, $P = 0.039$), but not in standard-risk patients (72 *vs* 80%, $P = 0.45$). CIF of CsA with a target level of 250–400 ng/ml may not be appropriate for GVHD prophylaxis in standard-risk patients.

Bone Marrow Transplantation (2004) **33,** 549–552. doi:10.1038/sj.bmt.1704374
Published online 12 January 2004
Keywords: hematopoietic stem cell transplantation; cyclosporine A; graft-versus-host disease; continuous infusion

Cyclosporine A (CsA) is a mainstay of treatment in the pharmacologic prevention of graft-versus-host disease (GVHD), and is usually combined with methotrexate (MTX). However, the dose, target blood level, and schedule of administration vary among protocols.[1] In particular, it has not been assessed whether CsA should be administered as a continuous infusion (CIF) or as twice-daily infusions (TD) in the early period after transplantation when patients cannot tolerate an oral intake. In September 1999, we changed the mode of CsA administration from TD to CIF, without major changes to other transplantation procedures. The aim of this study was to evaluate the impact of these two different modes of administration on the incidence of acute GVHD.

Correspondence: Dr Y Kanda, Department of Cell Therapy and Transplantation Medicine, University of Tokyo, 7-3-1 Hongo, Bunkyo-ku, Tokyo 113-8655, Japan; E-mail: ycanda@umin.ac.jp
Received 09 April 2003; accepted 05 July 2003
Published online 12 January 2004

Patients and methods

Patients

We retrospectively analyzed the records of adult patients who underwent allogeneic hematopoietic stem cell transplantation for the first time between June 1995 and May 2000 using a GVHD prophylaxis regimen consisting of CsA and MTX. During that time, this combination was the standard regimen for GVHD prophylaxis in our center, but CsA alone was used for patients who were at a very high risk for relapse, and a combination of tacrolimus and MTX was used for patients who had received a graft from an unrelated donor with at least one allele or antigen mismatch. Those who received a T-cell-depleted graft and those who received a reduced-intensity conditioning regimen or a conditioning regimen that included ATG or CAMPATH1-H were excluded. Otherwise, consecutive patients were included in the study. The data for 129 patients were analyzed. There were 95 males and 34 females with a median age of 38 years (range 18–60). Bone marrow (BM) was exclusively used in unrelated transplants, whereas 13 related donors chose a collection of G-CSF-mobilized peripheral blood stem cells (PBSC) rather than a BM harvest. BM was additionally harvested from poor mobilizers.

Transplantation procedure

Conditioning was mainly a combination of cyclophosphamide (60 mg/kg for 2 days) with either busulfan (4 mg/kg/day for 4 days) or total body irradiation (TBI; 2 Gy twice daily for 3 days). GVHD prophylaxis was with CsA and short-term MTX (10–15 mg/m^2 on day 1 and 7–10 mg/m^2 on days 3 and 6, and optionally on day 11), with a starting dose of CsA of 3 mg/kg/day. Before September 1999, CsA was administered as a 4 h infusion twice daily in equally divided doses. The dose of CsA was adjusted to maintain the trough blood CsA concentration between 150

and 300 ng/ml. After September 1999, CsA was administered as a CIF. The dose of CsA was adjusted to maintain the blood CsA concentration between 250 and 400 ng/ml. CsA concentration was measured at least once a week by fluorescence polarization immunoassay with a specific monoclonal antibody, using whole blood samples.[2] Metabolites of CsA were not measured by this method. The route of CsA administration was converted to oral at a ratio of 1:2 or 1:3 when patients were able to tolerate oral intake at least 3 weeks after transplantation. Acute GVHD was graded as previously described.[3] Prophylaxis against bacterial, fungal, and pneumocystis carinii infection consisted of fluconazole, tosufloxacin, and sulfamethoxazole/trimethoprim. As prophylaxis against herpes simplex virus infection, acyclovir was given from day −7 to 35. Pre-emptive therapy for cytomegalovirus infection was with ganciclovir, while monitoring cytomegalovirus antigenemia.[4]

Statistical considerations

Standard-risk disease was defined as acute leukemia in complete remission, chronic myelocytic leukemia in the first chronic phase, chemosensitive lymphoma, and myelodysplastic syndrome comprising refractory anemia or refractory anemia with ringed sideroblasts, while others were considered high-risk diseases. Renal dysfunction was defined as an elevation in serum creatinine level to above $\times 1.5$ or $\times 2.0$ the baseline value, except for that clearly caused by the administration of amphotericin B. Patients who received both BM and PBSC grafts were included in the PBSC group.

Probabilities and continuous variables in the two groups were compared using Fisher's exact test and the Mann–Whitney *U*-test, respectively. Cumulative incidences of acute GVHD and relapse were calculated using Gray's method, considering death without acute GVHD or relapse, as a competing risk.[5] Disease-free survival was estimated using the Kaplan–Meier method. Potential confounding factors considered in the analysis were age, sex, donor type (related or unrelated), stem cell source (BM or PBSC), disease risk, conditioning regimen, HLA mismatch, total dose of MTX, and mode of CsA administration.

Results

Patient characteristics

Of the 129 patients analyzed, 58 and 71 patients were in the TD and CIF groups, respectively. The CIF group included a significantly higher proportion of patients with high-risk disease ($P=0.021$), those transplanted from an unrelated donor ($P=0.004$), those who received an HLA-mismatched graft ($P=0.023$), and those who received a PBSC graft ($P=0.0061$) (Table 1). The total dose of MTX was significantly lower in the CIF group (median dose 35 mg/m^2 *vs* 33 mg/m^2, $P=0.0002$). Other characteristics were equivalent between the two groups.

Risk factors for grade II-IV acute GVHD

First, we performed a univariate analysis to evaluate the impact of potential confounding factors on the incidence of grade II–IV acute GVHD. As shown in Table 2, transplant from an unrelated donor, the presence of HLA mismatch, the use of a TBI-containing regimen, a lower total dose of MTX, and CIF of CsA were identified as significant risk factors for the development of grade II–IV acute GVHD. The incidence of grade II-IV acute GVHD in the CIF group (56%) was significantly higher than that in the TD group (27%, $P=0.00022$, Figure 1). Next, we performed a multivariate analysis using the backward stepwise selection method to identify independent risk factors for the development of grade II-IV acute GVHD. Only two factors, CIF of CsA (relative risk 2.59; 95% CI 1.46–4.60, $P=0.0011$) and the presence of HLA mismatch (2.01; 95% CI 1.15–3.53, $P=0.014$), were identified as independent significant risk factors (Table 3A). The impact of these two factors was significant even when adjusted for the total dose of MTX and donor type (Table 3B).

Table 1 Characteristics of the patients

	TD group (n = 58)	*CIF group (n = 71)*	*P-value*
Sex			
Male	42	53	0.84
Female	16	18	
Age			
<40 years	36	36	0.22
⩾40 years	22	35	
Risk			
Standard	39	33	0.021
High	19	38	
Donor			
Related	42	33	0.004
Unrelated	16	38	
HLA			
Match	50	9	0.023
Mismatch	8	22	
Stem-cell BM	57	59	0.0061
PBSC	1	12	
Regimen non-TBI	19	17	0.33
TBI	39	54	0.33

[a]BM = bone marrow, PBSC = peripheral blood stem cell, TBI = total body irradiation.

Renal toxicity

Renal dysfunction was significantly less frequent in the CIF group than the TD group: 27% *vs* 66% ($P<0.0001$) and 13% *vs* 41% ($P=0.0002$), when we defined renal dysfunction as an elevation of the serum creatinine level to above $\times 1.5$ and $\times 2.0$ the baseline value, respectively (Table 4).

Actual daily dose of CsA

We adjusted the dose of CsA to maintain the target blood level as described above. We compared the actual daily dose of CsA, excluding patients who were converted to oral administration. The actual daily dose of CsA in the CIF